Beamline 10.0.1

Photoemission of Highly Correlated Materials; High-Resolution Atomic, Molecular, and Optical Physics

Breakdown of the Franck-Condon approximation in N_2

Canton, S.E., J.D. Bozek, N. Berrah

Correlated processes in the inner-shell photodetachment of the Na^- ion

Covington, A.M., A. Aguilar, V.T. Davis, I. Alvarez, H.C. Bryant, C. Cisneros, M. Halka, D. Hanstorp, G. Hinojosa, A.S. Schlachter, J.S. Thompson, D.J. Pegg

Dynamical relativistic effects in photoionization: Spin-orbit-resolved angular distributions of xenon *4d* photoelectrons near the Cooper minimum

Hemmers, O., H. Wang, G. Snell, M.M. Sant' Anna, I. Sellin, N. Berrah, D.W. Lindle, P.C. Deshmukh, N. Haque, S.T. Manson

Electronic structure of divalent hexaborides

Denlinger, J.D., G.-H. Gweon, J.W. Allen, Z. Fisk

Experimental evidence of a dynamic Jahn-Teller effect in $D_{3d}C_{60}^+$

Canton, S.E., A. J. Yencha, M.C.A. Lopes, E. Kukk, J.D. Bozek, G. Snell, N. Berrah

Fermi surface topology, bilayer splitting, and (π,0) dispersion kinks in Bi2212

Gromko, A.D., Y.-D. Chuang, A.V. Fedorov, J.D. Koralek, Y. Aiura, Y. Yamaguchi, K. Oka, Y. Ando, D.S. Dessau

High resolution photoionization measurements of Mg^+ and Al^+ ions

Aguilar, A., J.B. West, R.A. Phaneuf, H. Kjeldsen, F. Folkmann, J.D. Bozek, A.S. Schlachter, C. Cisneros

K-shell photodetachment of Li^-: Experiment and theory

Bozek, J.D., A.A. Wills, G. Turri, G. Akerman, B. Rude, H.-L. Zhou, S.T. Manson, N.D. Gibson, C.W. Walter, L. Vo Ky, A. Hibbert, R.A. Phaneuf, S.M. Ferguson, N. Berrah

K-shell photoexcitation of carbon ions: lifetime of a K-shell vacancy

Schlachter, A.S., M.M. Sant' Anna, A.M. Covington, A. Aguilar, M.F. Gharaibeh, G. Hinojosa, R.A. Phaneuf, I. Alvarez, C. Cisneros, A. Müller, B.M. McLaughlin

Mirroring doubly excited resonances in neon

Canton, S.E., A.A. Wills, T.W. Gorczyca, M. Wiedenhoeft, E. Sokell, J.D. Bozek, G. Turri, X. Feng, N. Berrah

Photoionization of C^{2+} ions

Müller, A., R.A. Phaneuf, A. Aguilar, M.F. Gharaibeh, A.S. Schlachter, I. Alvarez, C. Cisneros, G. Hinojosa, B.M. McLaughlin

Photoionization of doubly charged scandium ions

Schippers, S., A. Müller, S. Ricz, M.E. Bannister, G.H. Dunn, J. Bozek, A.S. Schlachter, G. Hinojosa, C. Cisneros, A. Aguilar, A. Covington, M. Gharaibeh, R.A. Phaneuf

Photoionization of Ne^+: An absolute benchmark for theory

Covington, A.M., A. Aguilar, I. Álvarez, J.D. Bozek, C. Cisneros, I.R. Covington, I. Dominguez, M.F. Gharaibeh, G. Hinojosa, B.M. McLaughlin, M.M. Sant' Anna, A.S. Schlachter, C.A. Shirley, R.A. Phaneuf

Transmission functions of a Scienta SES-200 hemispherical analyzer

Canton, S.E., J.D. Bozek, N. Berrah

Vibrationally resolved resonant Auger spectroscopy of formaldehyde at the C $1s^{-1}$ π^* resonance

Bozek, J.D., S.E. Canton, E. Kukk, N. Berrah

BREAKDOWN OF THE FRANCK-CONDON APPROXIMATION IN N_2

S.E. Canton[1,2], J.D. Bozek[1] and N. Berrah[2]
[1] Lawrence Berkeley National Laboratory, Advanced Light Source,
University of California, Berkeley CA 94720.
[2] Department of Physics, Western Michigan University, Kalamazoo MI 49008.

INTRODUCTION

When a molecular electron is excited or ionized, it moves in a different charge distribution exerting in turn a different force on the nuclei. The nuclei respond by breaking into stronger vibrations. Electronic transitions are accompanied by vibrational transitions, which are called vibronic. The determination of which vibrations are stimulated is based on the view that nuclei move much faster than electrons, and so the rearrangement occurs in a virtually static nuclear frame. The Franck-Condon principle is the approximation that the nuclear conformation readjusts after the electronic transition, and not during it. The most probable conformation of the molecule when the transition begins is at the nuclei equilibrium position. At the end of the transition, the nuclei are still in their original position and this is the origin of the term vertical transition. The intensity of a transition between vibronic states depends on the magnitude of the transition moment. In the frame of the Franck-Condon approximation, it can be written as:

$$<\varepsilon'\nu'|\mu|\varepsilon\nu> = \mu_{\varepsilon'\varepsilon} * S_{\nu\nu'}$$

$S_{\nu\nu'}$ is the so-called Franck-Condon factor. It can then be seen that the ratio between two vibrational levels in the same electronic band should be constant.

Vibrational level intensity ratios as a function of photon energy have been determined in the valence spectrum of N_2 from 20-400 eV using photoelectron spectroscopy. Results for the B state show a large deviation from the Franck-Condon approximation and qualitatively agree with some recent fluorescent results [1,2].

EXPERIMENT

The experiment was conducted on beamline 10.0.1 at the ALS using a Scienta SES-200 hemispherical analyzer. The transmission function of the spectrometer was accounted for before extracting the gaussian fits of the peaks areas.

RESULTS

Vibrationally resolved photoelectron cross-sections of simple molecules were obtained close to threshold to explore the dynamical effects of shape resonances and Cooper minima on photoionization cross sections using 2nd generation light sources. Experimental resolution limitations made it impossible to extend those measurements beyond 40 eV. Recently, however, a recent experiment [1,2] was carried out to access vibrationally resolved photoionization data over a much wider spectral range using dispersed fluorescence from the residual photoion. Vibrational level population distributions of N_2^+ photoions in the $B^2\Sigma_u^+$ electronic state were probed by detecting the fluorescence emitted as they decayed into the $X^2\Sigma_g^+$ ionic state. Results for the B state shows a large deviation from the Franck-Condon approximation. We report in this work a *direct* similar study of this effect using photoelectron spectroscopy of these vibrational

levels population was conducted in the present experiment. Vibrational level intensity ratios as a function of photon energy were determined from 20-400 eV and are displayed in Fig.1 for the X state, in Fig.2 for the A state and in Fig.3 for the B state. Results for the B state show a large deviation from the Franck-Condon approximation consistent with the fluorescent results.

A complete analysis of the results is currently underway.

REFERENCES

[1] Rao et al, Phys. Rev. Lett. **76**, 2666 (1996).
[2] Prof. E. Poliakoff (private communication).

ACKNOWLEDGEMENT

Prof E. Poliakoff is greatly acknowledged for making the fluorescence data available.

This work was funded by the Department of Energy, Office of Science, Basic Energy Sciences, Chemical and Material Science Division, under the contract No. DE-AC03-76SF00098.

Principal investigator: Nora Berrah, Physics Dept., Western Michigan University, 616-387-4955, berrah@wmich.edu.

Fig. 1 Branching ratio v_1/v_0 for the X state as a function of photon energy.

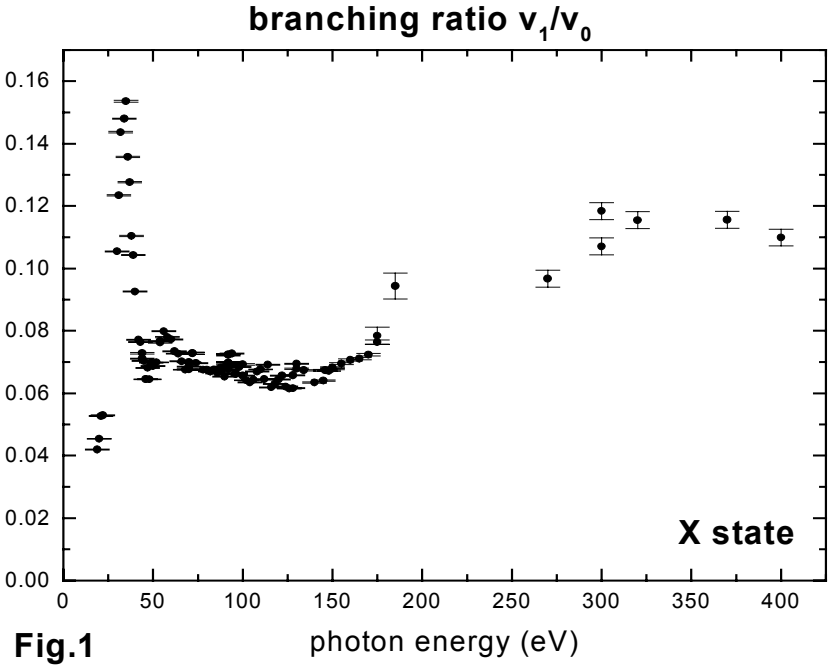

Fig.1

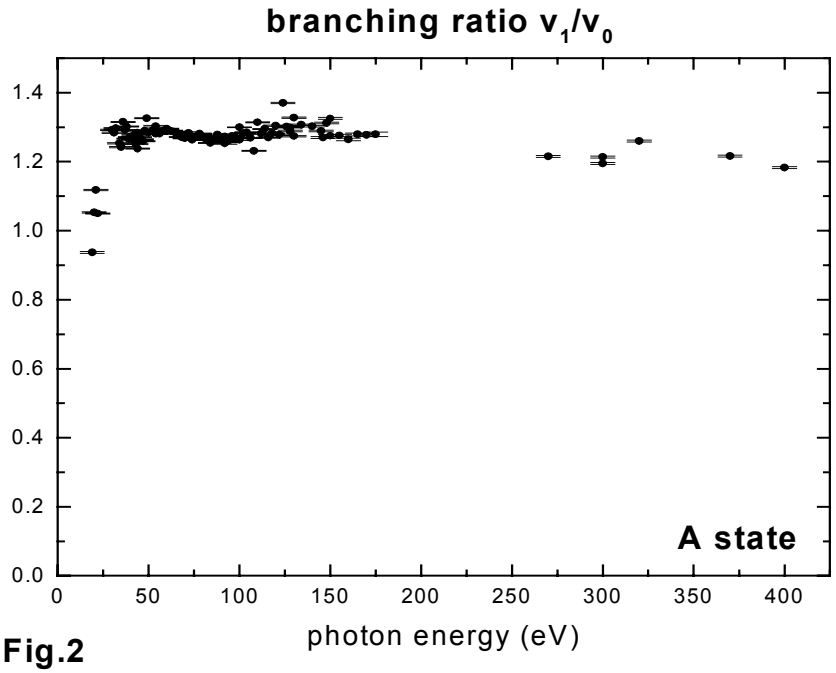

Fig.2 Branching ratio v_1/v_0 for the A state as a function of photon energy.

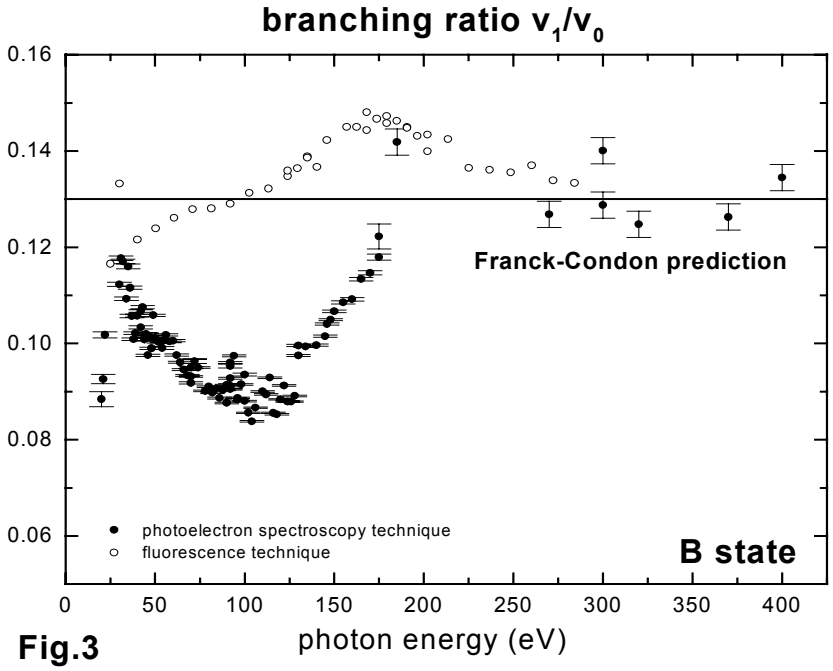

Fig.3 Branching ratio v_1/v_0 for the B state as a function of photon energy compared with fluorescence data (open circles).

Correlated Processes in the Inner-Shell Photodetachment of the Na^- Ion

A. M. Covington[1], A. Aguilar[1], V. T. Davis[2], I. Alvarez[3], H. C. Bryant[4], C. Cisneros[3], M. Halka[5], D. Hanstorp[6], G. Hinojosa[3], A. S. Schlachter[7], J. S. Thompson[1]and D. J. Pegg[8]

[1]Department of Physics and Chemical Physics Program,University of Nevada, Reno, Nevada 89557-0058, USA
[2]Department of Physics, United States Military Academy, West Point, NY 10996, USA
[3]Centro de Ciencias Fisicas UNAM, Apdo. Postal 48-3 CP 62251 Cuernavaca , Mor. Mexico
[4]Physics and Astronomy, University of New Mexico, Albuquerque, NM 87131, USA
[5]Department of Physics, Portland State University, P.O. Box 751, Portland, Oregon 97229, USA
[6]Department of Physics, Chalmers University of Technology and Goteborg University, SE-412 96 Goteborg Sweden
[7]Lawrence Berkeley National Laboratory, 1 Cyclotron Road, Berkeley, CA 94720, USA
[8]Department of Physics, University of Tennessee, Knoxville, TN 37996, USA

Photodetachment studies of negative ions have, until recently, involved the valence electrons only. Double excitation, a clear sign of the importance of electron correlation, has been investigated extensively during the past few decades[1]. Such measurements used lasers as the source of UV photons. At much higher levels of excitation, one can expect to observe thresholds and resonances in the photodetachment cross section arising from the detachment and/or excitation of an inner-shell electron. To reach these high levels of excitation, which in the present case lie in the XUV region, it is necessary to replace lasers with a synchrotron radiation source. The present experiment was performed on the photon-ion endstation 10.0.1.2 at the 10.0.1 beamline at the Advanced Light Source.

In the experiment we collinearly overlapped a beam of Na^- ions from a low-energy accelerator with a beam of XUV photons from the ALS. Na^- ions were produced in a sputter ion source, extracted at an energy of 5 keV and focused using a series of cylindrical electrostatic lenses. The ion beam was momentum-selected using a 60^o analyzing magnet. The cross sectional area of the ion beam was defined by two sets of adjustable slits. After momentum-selection and collimation, the ion beam was merged onto the axis of a counter-propagating photon beam using a set of 90^o spherical-sector bending plates. The primary beam then entered a 29.4 cm long cylindrical interaction region which was biased at +2 kV to energy label the Na^+ ions produced as a result of the photon-ion interactions. The energy labeling of these photo-ions enabled us to distinguish them from the Na^+ ions produced in double detachment collisions of the Na^- ions with the residual gas along the unbiased region of the ion beam line. This background contribution was also reduced by maintaining a vacuum of $5x10^{-10}$ Torr in the beam line. After the interaction region, a 45^o analyzing magnet was used to separate the energy-labeled Na^+ ions produced in the biased interaction region from the primary Na^- ion beam. These ions had an energy of 9 keV, whereas most of the collisionally detached background ions had an energy of 5 keV, as determined by the extraction voltage at the ion source. Typical Na^- ion currents in the interaction region were 1-6 nA. The magnitudes of the ion current and photon intensity were monitored for normalization purposes. The photon beam was modulated at 1 Hz in order to discriminate against the collisionally-induced background of 9 keV Na^+ ions produced in the interaction region. The Na^+ photo-ions were further deflected, in the vertical dispersion plane, by the use of a set of 90^o spherical-sector bending plates. This was to minimize any background arising from the collection of the Na^- primary beam. The dispersed Na^+ photo-ions then entered a negatively-biased detection box, where the ions impinged on a metal plate and produced secondary electrons. These secondary electrons were, in turn, accelerated toward a microchannel plate detector. The processed pulses from this detector were counted with a multi-function I/O board in a PC-based data acquisition and control system. The Na^+ signal, which is proportional

to the cross section, is shown, as a function of photon energy, in Figure 1. This figure is made up of two data sets taken under different conditions and smoothed separately. In the range 30-40 eV, the resolution and step size were 40 meV and 6 meV, respectively. In the range 40-51 eV the resolution and step size were both 100 meV. Further details can be found in a recent publication [2].

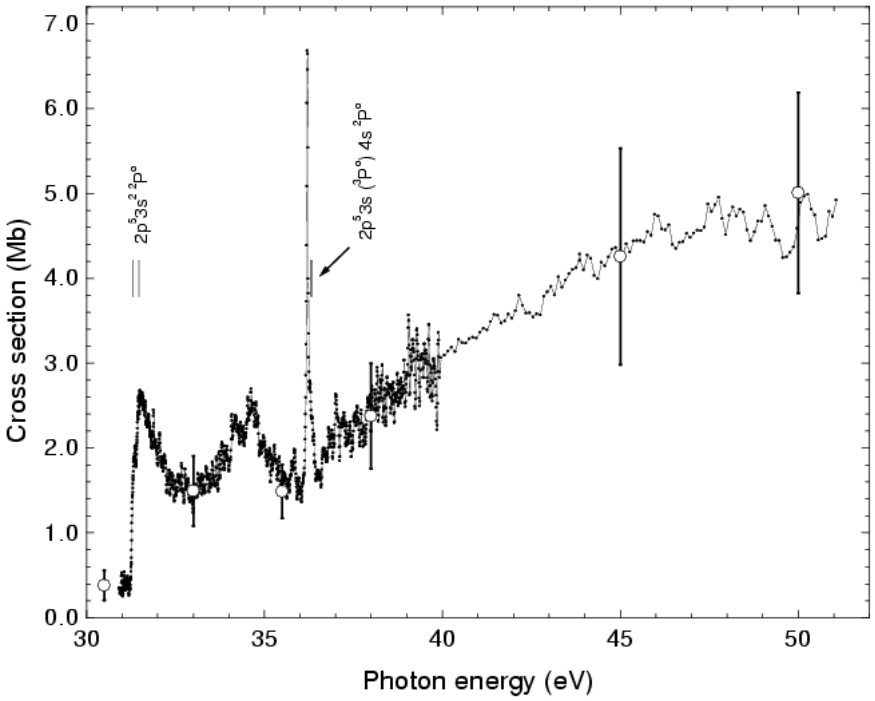

Figure 1 Total cross section for photodetachment of Na^- over energy range 30-51 eV. The six measurements represented by open circles were used to establish the cross-section scale. The scale shown is a lower limit. Thresholds are indicated by vertical lines.

Figure 1 shows the photodetachment cross section of the Na^- ion leading to the production of the Na^+ ion. In the measured energy range 30-51 eV, two distinct processes contribute to the cross section. There is the non-resonant process involving the direct photodetachment of a 2p electron from Na^- producing Na atoms in core-excited states, which rapidly decay via Auger emission to form Na^+ ions. The first channel to open is the $Na(2p^5 3s^2)^2P^o + e^-$ channel. The fine structure channels associated with the $^2P^o$ levels can be clearly seen. The sharp opening of this channel is expected for dominant s-wave emission. This channel is the most prominent non-resonant channel over the energy range studied. The cross rises gradually from threshold to a maximum slightly beyond the range of our measurements. At higher energies, detachment of the 2p electron is often accompanied by the excitation of a valence electron. Resonant processes are also apparent in the cross section. The resonances arise from photoexcitation of core-excited states of the Na^- ion of $^1P^o$ symmetry, which subsequently decay via autodetachment to corresponding core-excited states of the Na atom. The excited Na atoms then decay via the Auger process to produce Na^+ ions. The probability of radiative decay to the bound states should be very small. The most prominent feature of the cross section in the

range studied is the Na^- resonance at 36.213 eV. This narrow peak lies very close to the threshold for the opening of the $Na(2p^5 3s(^3P^o)4s)^2P^o + e^-$ channel. It is most likely associated with the autodetaching decay of a core-excited $^1P^o$ state of Na^- with a major configuration of the type $2p^5 3s4snl$, where l is even. The resonance appears to be just below the parent threshold. Feshbach resonances, such as this, are known to narrow as they approach their parent threshold. The strength of the prominent Na^- resonance, in comparison to corresponding resonances in Na, clearly demonstrates the much higher degree of correlation associated with double excitation process in the negative ion than in the atom. Other, weaker resonances, have been observed in the cross section. Details can be found in reference [2].

We would like to take this opportunity to thank Professor Ronald Phaneuf for permitting us to use the collinear beams apparatus situated at the 10.0.1.2 endstation at ALS. This apparatus was constructed at the University of Nevada, Reno under the direction of Dr Phaneuf. The work at ALS is supported by the US Department of Energy under contract DE-AC03-76SF00098. We would like to acknowledge support of A.C. and A.A. and the endstation by the Division of Chemical Sciences, Biosciences and Geosciences of the US Department of Energy under contract DE-FG03-ER14787 with the U. Nevada, Reno. I.A., C.C., G.H., and A.A. acknowledge support from DGAPA-UNAM and CONACyT. D.H acknowledges support from the Swedish Research Council. We would like to thank Brendan McLaughlin for valuable discussions.

References

[1]. For example, P.Harris et al., Phys. Rev.A 42,6443(1990); G.Haeffler et al., Phys. Rev. A 59, 3655(1999); I.Kiyan et al., Phys. Rev. Letters, 81, 2874 (1998).
[2]. A.M.Covington et al., J.Phys.B 34, L735(2001).

Contact Information:

Dr. David J. Pegg
401 Nielsen Physics Building
The University of Tennessee
Knoxville, TN 37996-1200
Phone: 865-974-7831
FAX: 865-974-7843
Email: djpegg@utkux.utk.edu

Dynamical Relativistic Effects in Photoionization: Spin-Orbit-Resolved Angular Distributions of Xenon 4*d* Photoelectrons near the Cooper Minimum

O. Hemmers,[1] H. Wang,[1,2] G. Snell,[3,4] M. M. Sant'Anna,[4] I. Sellin,[5] N. Berrah,[3]
D. W. Lindle,[1] P.C. Deshmukh,[6,7,8] N. Haque,[9] and S. T. Manson[7]
[1]Department of Chemistry, University of Nevada, Las Vegas, NV 89154-4003
[2]Department of Physics, Uppsala University, Box 530, S-751 21 Uppsala, Sweden
[3]Department of Physics, Western Michigan University, Kalamazoo, MI 49008-5151
[4]Advanced Light Source, Lawrence Berkeley National Laboratory, Berkeley, California 94720, USA
[5]Department of Physics, University of Tennessee, Knoxville, TN 37996
[6]Department of Physics, Indian Institute of Technology-Madras, Chennai 600036, India
[7]Department of Physics and Astronomy, Georgia State University, Atlanta, GA 30030
[8]Center for Theoretical Studies of Physical Systems, Clark-Atlanta University, Atlanta, GA 30314
[9]Department of Physics, Morehouse College, Atlanta, GA 30314

INTRODUCTION

Relativistic effects in atoms have long been known to be important for photoionization dynamics at high **Z** [1,2]. At low and intermediate **Z**, where the predominant effect of relativity has been thought to be spin-orbit splitting of states into $j=l\pm1/2$ with differing threshold energies [1], recent advances in experiment [3] and theory [4] have demonstrated observable consequences of relativistic effects on photoionization dynamics. One of the most sensitive dynamical quantities in photoionization is the energy of a Cooper minimum, where the dipole matrix element for a particular channel goes through (or nearly goes through) zero. Relativistic interactions were predicted to significantly affect Cooper minima two decades ago [2]. Here, we report on a combined experimental and theoretical study of 4*d* photoionization in Xe where the spin-orbit components $4d_{5/2}$ and $4d_{3/2}$ are individually resolved. Experimentally this is difficult in the energy region of the $4d\rightarrow\varepsilon f$ Cooper minima because the dominant $d\rightarrow f$ contribution to the cross section is very small. In the absence of dynamical effects due to relativistic interactions, Cooper minima for $4d_{5/2}$ and $4d_{3/2}$ photoionization will be located at the same *kinetic energy*. Consequently, $\beta_{5/2}$ and $\beta_{3/2}$ would be identical as a function of photoelectron energy. However, the present measurements clearly exhibit differences in the β parameters and confirm the long-untested theoretical prediction of Kim *et al.* [2]. Furthermore, $\beta_{5/2}$ and $\beta_{3/2}$ differ not only in the immediate vicinity of the Cooper minima, but over a broad energy region, demonstrating the importance of relativistic effects in the photoionization of intermediate-**Z** atoms over a much larger energy range than previously suspected. The $4d\rightarrow\varepsilon f$ non-relativistic Cooper minimum splits into three minima relativistically; $4d_{5/2}\rightarrow\varepsilon f_{5/2}$, $4d_{5/2}\rightarrow\varepsilon f_{7/2}$ *and* $4d_{3/2}\rightarrow\varepsilon f_{5/2}$. Each would appear at the same photoelectron energy in the absence of dynamical effects resulting from relativistic interactions.

EXPERIMENTS

To check possible systematic errors related to a particular experimental method, the measurements were done independently with hemispherical and time-of-flight (TOF) electron spectrometers at two different undulator beamlines at the Advanced Light Source (ALS) at Lawrence Berkeley National Laboratory. One experiment was carried out at beamline 10.0.1 using an endstation designed for gas-phase angle-resolved studies based on the Scienta SES-200 hemispherical electron analyzer (HEA) [5]. The analyzer is rotatable in the perpendicular plane,

allowing electron angular-distribution studies. Measurements at the θ angles of 0°, 54.7° and 90° were performed, and angular-distribution parameters were determined. In the TOF measurements, performed at ALS beamline 8.0, two analyzers are mounted in the perpendicular plane at θ=0° and θ=54.7°, allowing simultaneous measurements for accurate determination of β parameters [6]. To determine β parameters, the data were calibrated with the Ne-2*s* photoline, which has a fixed β value of 2. In both experiments, for most of the data, the photon energy was increased in 2-eV steps, because the energy splitting of the spin-orbit components is 2.0 eV. This approach permitted the measurement of $\beta_{5/2}$ and $\beta_{3/2}$ at the same photoelectron *kinetic energy*, and the difference $\beta_{3/2}$-$\beta_{5/2}$ could be calculated easily. At higher energies, where larger energy steps were used (TOF measurements only), continuous curves were interpolated through the measured values of β and used to estimate the difference $\beta_{3/2}$-$\beta_{5/2}$.

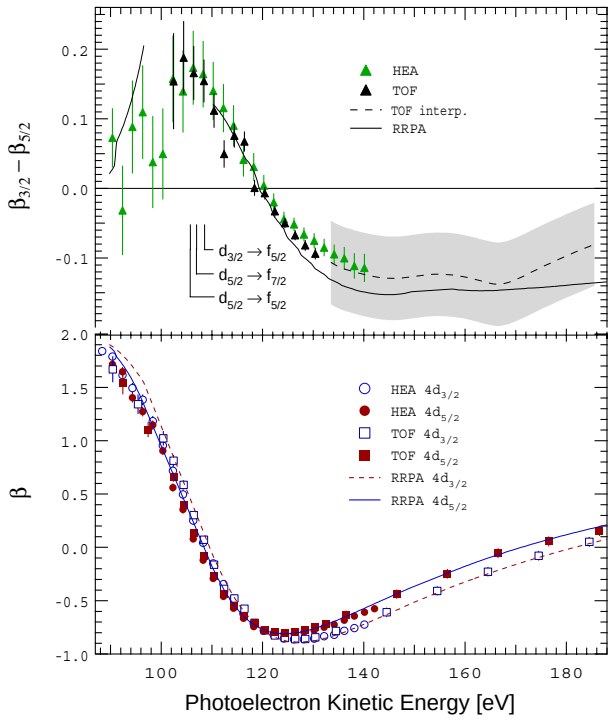

Figure 1. Lower panel: Photoelectron angular-distribution parameters, $\beta_{5/2}$ and $\beta_{3/2}$, for Xe 4*d* ionization as a function of photoelectron energy. The points are the present experiment and the curves are our theoretical results. Upper panel: $\beta_{3/2}$-$\beta_{5/2}$ as a function of photoelectron energy derived from the data in the lower panel. The dashed curve was obtained via interpolation of the TOF data, and the shaded area represents error bars. Omitted from theory is the region of the $4p \rightarrow ns,nd$ resonances. Also shown are theoretical predictions for the locations of the Cooper minima.

RESULTS

Calculations were performed using the relativistic random-phase approximation (RRPA) [7] based upon the Dirac Equation; relativistic effects are included on an *ab initio* basis. All relativistic single-excitation channels from the 4*s*, 4*p*, 4*d*, 5*s* and 5*p* subshells were included in the calculation, a total of 20 interacting channels. As noted above, in the absence of relativistic effects, β_j *must* be independent of j as a function of photoelectron energy. The present results for $\beta_{5/2}$ and $\beta_{3/2}$ as a function of photoelectron energy are shown in the lower panel of Fig. 1, where a clear difference is evident. To focus on this difference more clearly, values of $\beta_{3/2}$-$\beta_{5/2}$ are shown in the upper panel of Fig. 1, where zero corresponds to the nonrelativistic expectation. Also shown in Fig. 1 are the results of our RRPA calculations. The agreement is remarkably good between theory and experiment. The part missing from the theoretical curve is the $4p \rightarrow ns,nd$ resonance region where the theoretical results are affected by autoionization. There is also excellent agreement between the two sets of experimental results, providing confidence in the reliability of the measurements. Note particularly that the β-parameter curves are not simply shifted, but have different shapes, *e.g.*, $\beta_{3/2}$ goes lower than $\beta_{5/2}$, and the differences persist to higher energy. At still higher energies, recent work has shown that interchannel interactions are pervasive and often dominant for most subshells of most atoms at most energies [8], so much so

that even the asymptotic form of the high-energy nonrelativistic photoionization cross section for non-*s*-states is altered. Thus, as long as 4*d* photoionization does not dominate the total cross section, significant interchannel interactions will modify the 4*d* transition amplitudes. But there is no reason to expect these interchannel interactions will modify each relativistic amplitude in the same way, *i.e.*, interchannel coupling will cause observable differences between $\beta_{3/2}$ and $\beta_{5/2}$ for *all* higher energies. Near threshold, it is also known $\beta_{3/2}$ and $\beta_{5/2}$ differ due to differing exchange interactions among the relativistic channels. Only in the shape-resonance region, 30-80-eV kinetic energy, are there no differences between $\beta_{3/2}$ and $\beta_{5/2}$, because the 4*d* cross section dominates here and the energy is high enough so exchange interactions are no longer important; interchannel interactions are negligible *only* in this narrow region. Thus, except for a small energy region near the 4*d* shape resonance, equality of $\beta_{3/2}$ and $\beta_{5/2}$ is the exception, not the rule.

CONCLUSIONS

Finally, there is no reason to suspect Xe 4*d* is a special case; the results found in this work should be quite general. We thus expect effects of relativistic interactions on interchannel coupling will be widespread over all intermediate-**Z** atoms. These effects also should be manifest in clusters, molecules, surfaces, and solids.

ACKNOWLEDGMENTS

The authors thank the staff of ALS for their support during the experiments.

REFERENCES

1. S. T. Manson, C. J. Lee, R. H. Pratt, I. B. Goldberg, B. R. Tambe, and A. Ron, Phys. Rev. A **28**, 2885 (1983).
2. Y. S. Kim, A. Ron, R. H. Pratt, B. R. Tambe and S. T. Manson, Phys. Rev. Lett. **46**, 1326 (1981).
3. G. S. Canton-Rogan, A. A. Wills, T. W. Gorczyca, M. Wiedenhöft, O. Nayandin, C. N. Liu and N. Berrah, Phys. Rev. Lett. **85**, 3113 (2000).
4. H. S. Chakraborty, A. Gray, J. T. Costello, P. C. Deshmukh, G. N. Haque, E. T. Kennedy, S. T. Manson and J.-P. Mosnier, Phys. Rev. Lett. **83**, 2151 (1999).
5. N. Berrah, B. Langer, A. Wills, E. Kukk, J. D. Bozek, A. Farhat and T. W. Gorczyca, J. Electron Spectrosc. & Relat. Phenom. **101-103**, 1 (1999).
6. O. Hemmers, S. B. Whitfield, P. Glans, H. Wang, D.W. Lindle, R. Wehlitz, and I. A. Sellin, Rev. Sci. Instrum. **69**, 3809 (1998).
7. W. R. Johnson and C. D. Lin, Phys. Rev. A **20**, 964 (1979).
8. D. L. Hansen, O. Hemmers, H. Wang, D. W. Lindle, I. A. Sellin, H. S. Chakraborty, P. C. Deshmukh and S. T. Manson, Phys. Rev. A **60**, R2641 (1999).

This work was supported by the DOE, Office of Science, BES, DOE EPSCoR, NSF, NASA and CNPq, Brazil. The ALS is funded by the DOE, Materials Sciences Division, Basic Energy Sciences, under Contract No. DE-AC03-76SF00098.

Principal investigator: Dennis Lindle, Department of Chemistry, University of Nevada, Las Vegas, NV 89154-4003. Email: lindle@unlv.edu. Telephone: 702-895-4426.

This work has been published in Phys. Rev. Lett. **87**, 123004 (2001).

Electronic Structure of Divalent Hexaborides

J. D. Denlinger[1], G.-H. Gweon[2], J. W. Allen[2] and Z. Fisk[3]
[1]Advanced Light Source, Lawrence Berkeley National Lab, Berkeley, California 94720, USA
[2]Department of Physics, University of Michigan, Ann Arbor, Michigan 48109, USA
[5]NHMFL, Florida State University, Tallahassee, Florida 32306, USA

INTRODUCTION

Great interest in the divalent hexaborides has been generated recently by the discovery of high Curie temperature weak-moment ferromagnetism (FM) in La-doped CaB_6 [1] and by exotic theoretical models to explain the unusual magnetism, *e.g.* that it represents the ground state of a dilute electron gas [2] or of a doped excitonic insulator [3]. The starting point of most thinking about the divalent hexaborides, and central to the excitonic instability model, is the presumed existence of a band overlap between the top of the boron valence states and the bottom of the cation *d*-conduction band at the X-point of the simple cubic Brillouin zone appropriate to these materials. Without such overlap stoichiometric divalent hexaborides would be insulators. Band overlap is predicted by band structure calculations [4] and magneto-oscillatory studies [5] have been interpreted in this semi-metal framework. However, a new quasiparticle band calculation that includes a GW self-energy correction predicts CaB_6 to have an X-point bandgap of 0.8 eV [6].

Our early angle-resolved photoemission spectroscopy (ARPES) studies at the SRC synchrotron of EuB_6 and SrB_6 showed, contrary to the band-overlap picture, an isolated X-point electron pocket separated from the X-point boron valence band maximum by a gap >1 eV. Motivated by the prior theoretical and experimental evidence for bulk band overlap and by certain surface sensitive aspects of the data, we interpreted the observed gap as a property only of the surface region probed in ARPES. The new quasiparticle band calculation provides a theoretical basis for interpreting the X-point bandgap as a bulk property of divalent hexaborides. Reported here are new ARPES measurements of CaB_6 and EuB_6 [7], that provide a more detailed view of the k-dependent electronic structure and variations of the surface chemical potential with cation and time.

EXPERIMENT

Single crystal samples of CaB_6 and EuB_6, grown from an aluminum flux using powders prepared by boro-thermally reducing cation oxides, were cleaved in ultra-high vacuum ($<4\times10^{-11}$ torr) at ≈30K exposing the [001] surface for ARPES measurements at ALS Beamline 10.0.1. The ability to rotate the HERS spectrometer relative to the incident beam polarization allowed for measurement in two different symmetry selection geometries, *i.e.* p- and s-polarization. A total instrumental resolution of ≈40 meV and full angular acceptance of ≈0.2° was employed.

RESULTS

Figures 1(a,b) show the experimentally measured band structure for CaB_6 along Γ-X for the two different p- and s-polarization geometries. The data exhibit strong initial state symmetry selection rule effects. Fig. 1(c) shows a sum of the two polarization data sets with comparison to the GW calculated band structure [6]. Identification of all the calculated bands in the summed data, but not for the individual polarizations, highlights the utility and importance of having this rotational capability of the HERS detector. The bands selected by the s-polarization geometry correspond to the theory bands labeled 2 and 5, both of which have the same symmetry label of Δ_5.

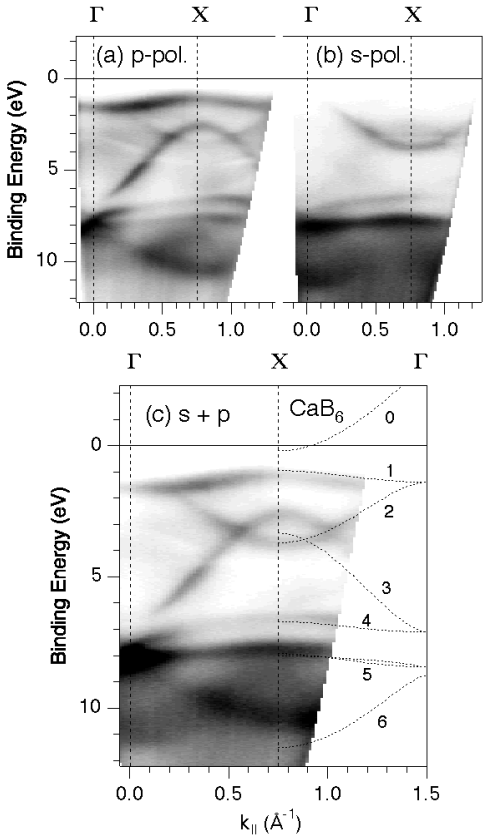

Fig. 1. Comparison of the experimental and theoretical band structures of CaB_6 along Γ-X. The reverse gray scale image of angle-resolved photoelectron intensities is the sum of two data sets with 30 eV s- and p-polarized excitation. Dashed lines are from the quasiparticle GW calculation [6] shifted by 0.45 eV to lower energy.

The qualitative agreement between experiment and theory dispersions in Fig. 1(c), most importantly including the existence of a band gap near E_F, is very striking. The theory bands have been rigidly shifted by 0.45 eV to lower energy for better visual alignment to the experimental data. Quantitative discrepancies, however, are also quite visible, including: *(i)* the size of the band gap near E_F, *(ii)* the overlap between bands 2 and 3, *(iii)* the overall boron-block bandwidth (between bands 1 and 6), and *(iv)* an additional weak broad dispersion at the bottom of the valence band.

This latter counter-dispersing band, 11 eV at Γ to ≈9 eV at X is suggestive of band back-folding resulting from a periodicity doubling. Indeed, low energy electron diffraction (LEED) images of freshly cleaved CaB_6 surfaces exhibit 2×1 surface order. The absence of conduction band intensity (band 0) at E_F for CaB_6 in Fig. 1 implies a >1 eV band gap and insulating behavior. While this result agrees with electron counting for stoichiometric material, it does not agree with bulk Hall transport measurements of electron carriers and dHvA measurement of Fermi surfaces. Also, as noted, earlier ARPES measurements of EuB_6 and SrB_6 both showed X-point electron pockets and ellipsoidal Fermi surface contours, contrary to this CaB_6 data set.

To address these different results for different cations, we present in Fig. 2 ARPES measurements along Γ-X for EuB_6 for the p-polarization geometry. Similar to the CaB_6 data in Fig. 2(a), the Δ_5 symmetry bands (2 and 5) are absent and no states near E_F are observed (see top panels of Fig. 2). However, this surface exhibited a very interesting time dependent behavior, illustrated by Fig. 2(b,c), in which the emergence of a small electron pocket at the X-point (corresponding to band 0 in Fig.1) is observed at ≈4 hours after cleavage of the sample. Accompanying this change at E_F, some additional redistribution of spectral weight in the boron block bands also occurs (illustrated by a comparison of X-point spectra in Fig. 2(c)). In addition, while the surface order before and after the spectral changes in this sample is not known, another important difference between EuB_6 and CaB_6 is the observation of 1×1 versus 2×1 LEED, respectively, performed after the ARPES experiments.

While the mechanism for this temporal change is not yet understood, it is important to note that the existence of the >1 eV X-point gap between bands 0 and 1 does *not* change — only the position of the chemical potential varies. Presumably band bending near the surface either relaxes an insulating surface layer or creates a metallic surface two-dimensional electron gas. The former is implied by bulk transport and dHvA measurements which show n-type carriers and the existence

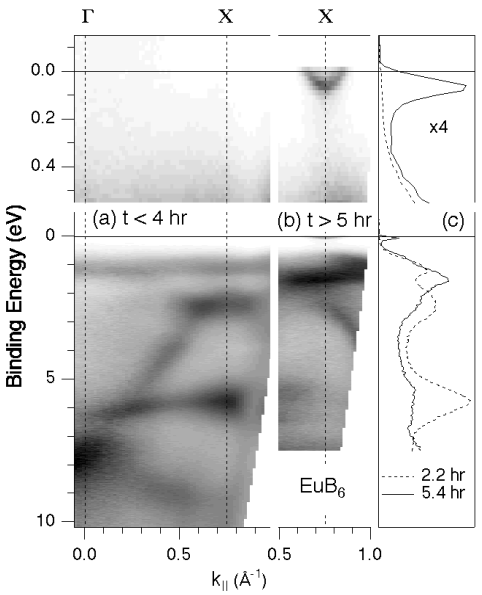

Fig. 2. Time dependent change in the band structure of EuB_6. (a) <4 hours and(b) >5 hours after the initial cleave. The reverse gray scale images are measured with p-polarized 30 eV excitation. (c) Comparison of X-point spectra. Upper panels show an expanded region near E_F.

of small elliptical Fermi surface pockets for the bulk electronic structure. The ability to simultaneously measure the complete band dispersions at the X-point using the angular mode of the Scienta analyzers was crucial to the discovery and monitoring of such time-dependent changes. Complementary bulk-sensitive soft x-ray absorption and emission measurements at the boron K-edge performed at ALS Beamline 8.0 [8] also provide an (angle-integrated) confirmation of the existence of a bulk band gap consistent with the ARPES data.

In summary, the existence of a semiconducting bandgap (rather than a semimetallic band overlap) is observed in the divalent hexaborides, thereby ruling out the excitonic insulator model for the novel FM in La-doped CaB_6. The location of the chemical potential at the bottom of conduction band indicates non-stoichiometric defects contributing excess electrons. The likely defects are boron vacancies, recently shown to carry magnet moments [9], and may be relevant to the novel ferromagnetism discovered in doped and undoped divalent hexaborides .

REFERENCES

1. D. P. Young *et al*, Nature **397**, 412 (1999).
2. D. Ceperley, Nature **397**, 386 (1999); G. Ortiz, M. Harris and P. Ballone, Phys. Rev. Lett. **82**, 5317 (1999).
3. M. E. Zhitomirsky, T. M. Rice, and V. I. Anisimov, Nature **402**, 251(1999); L. Balents and C. M. Varma, Phys. Rev. Lett. **84**, 1264 (2000); V. Barzykin and L. P. Gor'kov, Phys. Rev. Lett. **84**, 2207 (2000).
4. A. Hasegawa and A. Yanase, J. Phys. C, Solid State Phys. **12**, 5431 (1979); S. Massidda, A. Continenza, T. M. D. Pascale, and R. Monnier, Z. Phys. B **102**, 83 (1997).
5. R. G. Goodrich *et al*., Phys. Rev. B **58**, 14896 (1998); M. C. Aronson *et al*., Phys. Rev. B **59**, 4720 (1999).
6. H. J. Tromp *et al*., Phys. Rev. Lett. **87**, 016401 (2001).
7. J. D. Denlinger *et al*., cond-mat/0107429.
8. J. D. Denlinger, G.-H. Gweon, J. W. Allen, A. D. Bianchi and Z. Fisk, cond-mat/0107426; Surface Review and Letters, in press; and ALS Compendium, 2001.
9. R. Monnier and B. Delley, Phys. Rev. Lett. **87**, 157204 (2001).

This work was supported at U. of Michigan by the U.S. Dept. of Energy (DoE) under contract No. DE-FG02-90ER45416 and by the U.S. NSF under grant No. DMR-99-71611.

Principal investigator: Jonathan Denlinger, Advanced Light Source, LBNL. Email: JDDenlinger@lbl.gov. Telephone: 510-486-5648.

Experimental evidence of a dynamic Jahn-Teller effect in D_{3d} C_{60}^+

S.E. Canton[1,2], A.J. Yencha[4], M.C.A. Lopes[5],
E. Kukk[3], J.D. Bozek[1] G.Snell[2] and N. Berrah[2]
[1] Lawrence Berkeley National Laboratory, Advanced Light Source,
University of California, Berkeley CA 94720.
[2] Department of Physics, Western Michigan University, Kalamazoo MI 49008.
[3] Department of Physical Sciences, Oulu University, Linnanmaa, Oulu FIN-90570, Finland.
[4] Department of Chemistry, State University of New-York at Albany, Albany NY 122222
[5] Departmento de Fisica, ICE, Universidade Federal de Juiz de Fora, Juiz de Fora-MG,
CEP 36036-330 Brazil.

INTRODUCTION

Since its discovery in 1985, C_{60} has been the subject of intense studies. Most of its astonishing properties can be explained by its particular electronic structure. However, very little is known about C_{60}^+, which is of great interest for astrophysics and solid state physics. Characteristics as fundamental as the shape of the cation are still under debate. Because of its high symmetry, C_{60}^+ experiences a Jahn-Teller distortion and the Born-Oppenheimer approximation commonly used to obtained adiabatic potential energy surfaces is not applicable in this case. A recent analytical model [2] predicts different equilibrium geometry depending on the electron-phonon coupling strength. The number of vibronic states is shown to be directly correlated to the geometry. We have recently measured the valence photoelectron spectrum of C_{60}. The three-peak structure of the Highest Occupied Molecular Orbital (HOMO) is clearly resolved and strongly supports a D_{3d} geometry for C_{60}^+ in its ground state.

EXPERIMENT

The experiment was performed on beamline 10.0.1 at the ALS. A resistively heated oven generated an effusive beam of C_{60}. The photoelectron spectra were recorded in a crossed beam configuration using a Scienta SES-200 hemispherical analyzer at the magic angle. The spectrometer was operated at 20 eV pass energy and the photon resolution was set to 10 meV.

RESULTS

Semi classical and ab-initio calculations agree to attribute H_u symmetry to the highest occupied molecular orbital (HOMO) of C_{60}. The JT active modes are then of h and g symmetry. As this outermost orbital is highly delocalized over the rigid frame of 60 carbon atoms, any distortion is supposed to be small and the resulting ionized states are going to be best described as originating from a dynamic JT effect. The corresponding static $H\otimes(h\oplus g)$ JT problem was investigated analytically [1]. Minimization of the adiabatic energy surface for this problem results in wells of either D_{5d} or D_{3d} symmetry depending on the coupling strength. The dynamic JT problem can then be solved in the tunneling regime [2] to find the I_h symmetrized combinations of the states associated with the wells. The findings are the following: if the coupling is very strong, the absolute minimum has a D_{3d} symmetry and there are 3 tunneling states of A (not degenerate), G (4 times degenerate) and H (5 times degenerate) symmetry. In the case of weaker coupling, the absolute minimum is of D_{5d} symmetry and there are 2 tunneling states of A and H symmetry.

The present analysis of the bandshape in photoelectron spectra recorded at the magic angle strongly supports the first experimental evidence of a D_{3h} equilibrium geometry. The fitting procedure with asymmetric gaussians (Fig 1). allows the extraction of 3 bands I, II and III of area in the 1:4:5 ratio, corresponding to the tunneling states. An attempt to model the envelope with only 2 underlying peaks fails to reproduce the overall shape and doesn't give the areas in the 1:5 ratio. This rules out the possibility of a D_{5h} geometry predicted by an INDO calculation [3] and raises the question of the validity of the perturbative approach often used to derive some of the properties of this material, as the D_{3h} geometry is the signature of a strong electron-phonon interaction [2].

REFERENCES

[1] A. Ceulemans, P.W. Fowler, J. Chem. Phys. **93**, 1221 (1990).
[2] C. P. Moate et al, J. Phys. Condens. Matter **9**, 6049 (1997).
[3] R.D. Bendale et al, Chem. Phys. Lett., **194**, 467 (1992).

ACKNOWLEDGEMENTS

M.C.A. Lopes gratefully acknowledges financial support from CNPq (Brazil)
This work was funded by the Department of Energy, Office of Science, Basic Energy Sciences, Chemical Science Division, under the contract No. DE-AC03-76SF00098.

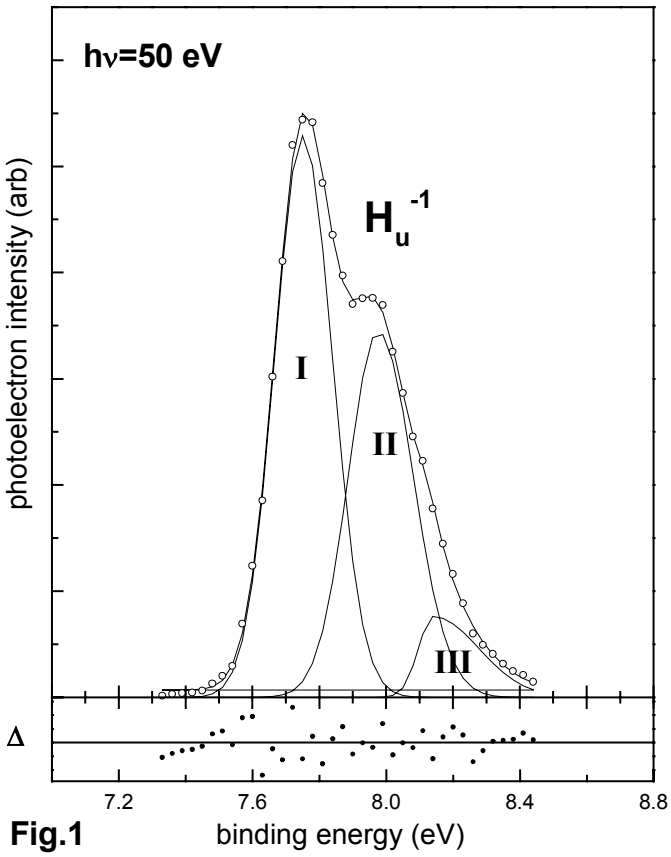

Fig.1

Fig.1: Fit of the HOMO band by three asymmetric gaussians. Δ indicates the difference between the data points and the fit.

This work was supported by the Director, Office of Science, Office of Basic Energy Sciences, of the U.S. Department of Energy under Contract No. DE-AC03-76SF00098.

Principal investigator: Nora Berrah, Western Michigan University. Email: berrah@wmich.edu. Telephone: 616-387-4955.

Fermi Surface Topology, Bilayer Splitting, and (π,0) dispersion kinks in Bi2212

A. D. Gromko[1],Y.-D. Chuang[1,2], A. V. Fedorov[1,2], J. D. Koralek[1], Y. Aiura[3], Y. Yamaguchi[3], K. Oka[3], Yoichi Ando[4], D. S. Dessau[1]

[1]Department of Physics, University of Colorado, Boulder, CO 80309-0390, USA
[2]Advanced Light Source, Lawrence Berkeley National Lab, Berkeley, CA 94720, USA
[3]National Institute of Advanced Industrial Science and Technology (AIST), AIST Tsukuba Central 2, 1-1-1 Umezono, Tsukuba, Ibaraki 305-8568, JAPAN
[4]Central Research Institute of Electric Power Industry (CRIEPI), 2-11-1 Iwato Kita, Komae, Tokyo 201-8511, JAPAN

INTRODUCTION

There have been many key developments in our understanding of the E vs. **k** band dispersion in $Bi_2Sr_2CaCu_2O_{8+\delta}$ (Bi2212) recently, both in the normal and superconducting states. Earlier work of ours [1] was the first to break tradition and indicate that the Fermi Surface (FS) of Bi2212 was not simply a single hole-like pocket centered around the (π,π) points of the Brillouin zone. In particular, we found that a more electron-like portion of the FS was observable at certain photon energies such as 33 eV, in contrast to the standard hole-like FS, which is observed at photon energies near 20 eV. Papers [2] and [3] dealt with this issue and principally contained data from the ALS. The concept of an electron-like FS portion in Bi2212 was supported by additional measurements made by the Stanford group [4]. This Fermi surface topology issue has evolved into the finding of bilayer split bands in the Bi2212 family [6,7]. This discovery explains the observance of two different FS topologies, and has allowed us to unearth new self-energy effects in the E vs. **k** band dispersion near the critical (π,0) point of the Brillouin zone [8,9].

EXPERIMENT

Experiments were carried out at beamline 10.0.1.1 of the Advanced Light Source, and at beamline 5-4 of the Stanford Synchrotron Radiation Laboratory using Scienta SES 200 electron spectrometers. Experiments were conducted at photon energies of 20, 22, 33, and 47eV. The measurements requiring the highest resolution were carried out with a combined experimental energy resolution of 12meV, and a momentum resolution better than $0.01\pi/a$ (where a is the CuO_2 plane lattice constant) along the entrance slit to the spectrometer. Experiments were carried out with the in-plane component of the photon polarization along the (0,0)-(π,0) direction.

RESULTS AND DISCUSSION

The bilayer splitting effect in Bi2212 is expected to occur due to the intracell c-axis coupling between the two CuO_2 layers per unit cell. However, this had not been previously observed, with most experiments indicating that the coupling was zero [5], a possibility consistent with exotic theories of superconductivity such as those favoring the low-dimensional state necessary for spin-charge separation. Simultaneous to the Stanford group's report [6], we made the first measurements of bilayer splitting in a high temperature superconductor, using overdoped Bi2212 samples [7]. We found the splitting to have a maximum value of approximately 100 meV, to be maximal at the (π,0) point of the Brillouin zone, and to be zero

along the (π,π) nodal direction. The large value of this splitting relative to other parameters such as the value of the superconducting gap, pseudogap, and some of the magnetic energy scales means that this intracell coupling is strong and should be included in any proper description of the electronic structure. This also should be necessary information for understanding why the T_c of the cuprates depends so strongly upon the number of layers per unit cell. Data showing this splitting is contained in figure 1.

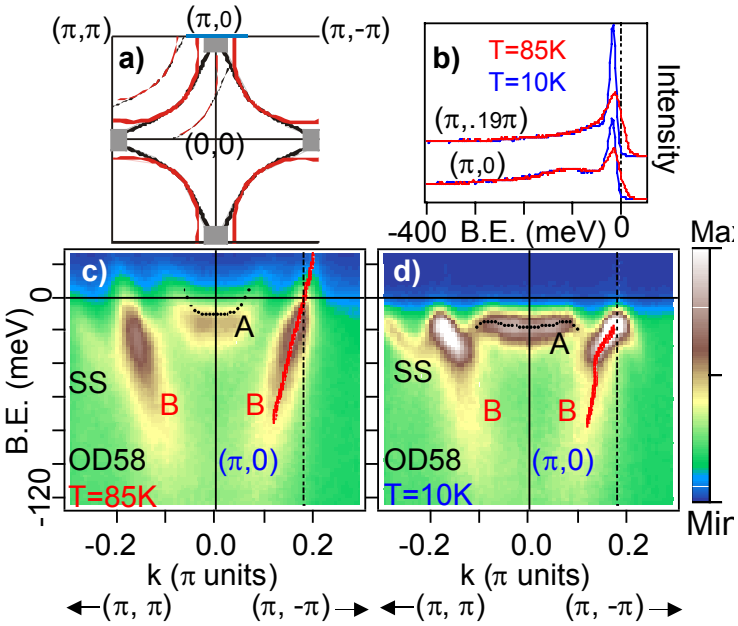

Figure 1. ARPES data in the normal (c) and superconducting state (d) of a T_c=58K overdoped Bi2212 sample, from ref [9]. A and B indicate the antibonding and bonding bands, respectively. The k-space location is along the blue line of panel (a). Panel (b) shows EDCs at two k-space locations.

A later paper of ours made the first extension of the bilayer splitting measurements to optimal and underdoped samples [8]. In these samples, the intrinsic peak broadening is greatly increased, and it is more difficult to separate the contributions of the separate bilayer split bands. By choosing optimal photon energy and polarization conditions we were able to selectively enhance one of the bilayer split bands relative to the other and make an accurate deconvolution. While the decreased c-axis conductivity in underdoped samples led us to expect that the bilayer splitting would be reduced in these samples as well, we found the surprising result that the bilayer splitting energetics are essentially identical for all doping levels [8]. This implies that other effects such as the scattering rate or the opening of the pseudogap must be more relevant to the change in the c-axis conductivity.

The ability to accurately deconvolve the bilayer splitting opened up many more opportunities for research in the critical (π,0) region of the Brillouin zone, where the bilayer splitting is the largest, as well as where the superconducting gap, pseudogap, van-Hove singularity, etc. are all maximal. Earlier measurements had been unknowingly looking at a superposition of the two bands in this region, with misinterpretations arising because of this. For example, there was the very famous peak-dip-hump lineshape at (π,0) observed by many groups in the superconducting state of Bi2212, but not in the normal state. This had been discussed as various types of self-energy effects, including $\alpha^2F(\omega)$ oscillations, coupling to magnetic modes, shake-off effects, etc. Our new data indicates that it is simply an effect of the bilayer splitting [9]. It is present in both the normal and superconducting states (figure 1b), but it was only previously visible in the superconducting state because the broad features present in the normal state pushed the signal below the background.

Even more importantly, the ability to accurately deconvolve the bilayer split bands has allowed us to make the first measurements of a dispersion "kink" near the (π,0) portion of the

Brillouin zone (figure 1d). This result follows up on the pioneering kink studies of cuprates done by the Stanford [10] and other [11,12] groups, except that these previous results were predominantly limited to the nodal region, where the pairing correlations are weakest. We have measured the temperature and momentum dependence of the new $(\pi,0)$ kink on over and optimally doped samples. We find that the kink strength (but not its energy scale) is a strong function of these parameters. In particular, the kink appears just below T_c, existing only in the superconducting state, while the nodal kink is present both above and below T_c. Also, the kink is localized in a small k-space region near $(\pi,0)$, with a momentum dependence that closely matches that of the famous "41 meV" magnetic resonance mode observed in inelastic neutron scattering measurements [13]. We argue that these factors point to a likely connection between the $(\pi,0)$ kink and the magnetic resonance mode, although more work needs to be done to understand the energy scales. If this picture holds together, the kink should be due to electronic coupling to the magnetic resonance and there will be a strong possibility that the pairing of electrons is mediated by this magnetic mode. This should be a very active and important area for future study.

ACKNOWLEDGEMENTS

We acknowledge sample preparation help from M. Varney, beamline support from X.J. Zhou, P. Bogdanov, Z. Hussain and D.H. Liu, and helpful discussions with G. Aeppli, A. Chubukov, C. Kendziora, A. Millis, P. Lee, D. Pines, D. Scalapino, J. Schmallian, Z-X. Shen, and S.C. Zhang. We gratefully acknowledge the help of R. Goldfarb at NIST for the use of the SQUID magnetometer.

REFERENCES

1. Y.-D. Chuang, A. D. Gromko, D. S. Dessau, Y. Aiura, Y. Yamaguchi, K. Oka , A. J. Arko, J. Joyce, H. Eisaki, S.I. Uchida, K. Nakamura, Yoichi Ando, Phys. Rev. Lett. **83** 3717, 1999.
2. A. D. Gromko, Y. -D. Chuang, D. S. Dessau, Y. Aiura, K. Oka, K. Nakamura, Yoichi Ando, cond-mat/0003017.
3. Y.-D. Chuang, A. D. Gromko, D. S. Dessau, K. Nakamura, Yoichi Ando, Physica C **341-348**, 2079 (2000).
4. D.L. Feng et al., cond-mat/9908056; P. Bogdanov et al, cond-mat/0005394.
5. H. Ding et al., Phys. Rev. Lett. **76**, 1533 (1996).
6. D.L. Feng, et al., Phys. Rev. Lett. **86**, 5550 (2001).
7. Y.-D. Chuang, A. D. Gromko, A.Fedorov, Y. Aiura, K. Oka, Yoichi Ando, H. Eisaki, S.I. Uchida, D. S. Dessau, Phys. Rev. Lett. **87**, 117002 (2001).
8. Y.-D. Chuang, A.D. Gromko, A.V. Fedorov, Y. Aiura, K. Oka, Yoichi Ando, D. S. Dessau cond-mat/0107002 (Phys Rev Lett, submitted).
9. A.D. Gromko, A.V. Fedorov, Y.-D. Chuang, J.D. Koralek, Y. Aiura, Y. Yamaguchi, K. Oka, Yoichi Ando, D. S. Dessau (in preparation).
10. A. Lanzara, P. V. Bogdanov, X. J. Zhou, S. A. Kellar, D. L. Feng, E. D. Lu, T. Yoshida, H. Eisaki, A. Fujimori, K. Kishio, J.-I. Shimoyama, T. Noda, S. Uchida, Z.Hussain, Z.-X. Shen, Nature **412**, 510 (2001).
11. A. Kaminski et al., Phys. Rev. Lett. **86**, 1070-1073 (2001).
12. P.D. Johnson et al., Phys. Rev. Lett. **87** 177007 (2001).
13. H. He et al. Phys. Rev. Lett. **86**, 1610-1613 (2001).

This work was supported by the NSF Career-DMR-9985492 and the DOE DE-FG03-00ER45809. ALS and SSRL are operated by the DOE, Office of Basic Energy Sciences.

Principal investigator: Dan Dessau, University of Colorado, Department of Physics, Boulder, CO 80309. Email: dessau@spot.colorado.edu. Telephone: 303-492-1607.

High Resolution Photoionization Measurements of Mg^+ and Al^+ Ions

A Aguilar[1,4], J B West[2], R A Phaneuf[1], H Kjeldsen[3], F Folkmann[3], J D Bozek[4], A S Schlachter[4] and C Cisneros[5]

[1]Department of Physics, MS220, University of Nevada, Reno, NV, 89557-0058, USA
[2]CLRC Daresbury Laboratory, Warrington WA4 4AD, UK
[3]Institute of Physics and Astronomy, University of Aarhus, DK-8000 Aarhus C, Denmark
[4]Advanced Light Source, Berkeley Lab, Berkeley, CA 94720, USA
[5]Centro de Ciencias Físicas, Universidad Nacional Autónoma de México, Apartado Postal 6-96, Cuernavaca 62131, México

INTRODUCTION

The measurements presented here were undertaken to provide high resolution data on the photoionization cross sections of the singly charged ions of Mg and Al. The initial measurements were made at the ASTRID storage ring at the University of Aarhus, where absolute cross sections were obtained, but the photon energy resolution was insufficient to identify all the spectral structure. This was particularly evident in regionswhere the $2p \rightarrow nd$ and ns resonances overlapped; configuration interaction was strong in these regions and it was difficult to make firm assignments. Beamline 10.0.1 at the ALS was able to provide resolution down to $\sim$5 meV in the photon energy region of interest, thereby revealing the underlying structure in the features observed previously [1, 2]. In this ALS experiment there was no requirement to make absolute measurements, since these had already been made on ASTRID. The present data could therefore easily be normalised to the earlier data to obtain oscillator strengths for the newly resolved structure.

EXPERIMENT

The measurements were made using the merged beam method, originally used for electron scattering cross sections [3] and later adapted for photoionization cross section measurements at the Daresbury Synchrotron Radiation Source [4]. At the ALS an ECR source was used to generate the ions of interest; it contained a metal vapour oven so that metallic ions could be produced. The ions were then magnetically selected and deflected electrostatically to merge with the path of the photon beam from a spherical grating monochromator over a length of $\sim$30 cm. The parent beam intensity was measured in a Faraday cup, and the ionised products were incident upon a stainless steel plate. The secondary electrons thus generated were detected by a microspherical plate; further details of the experimental equipment have been given by Covington *et al* [5].

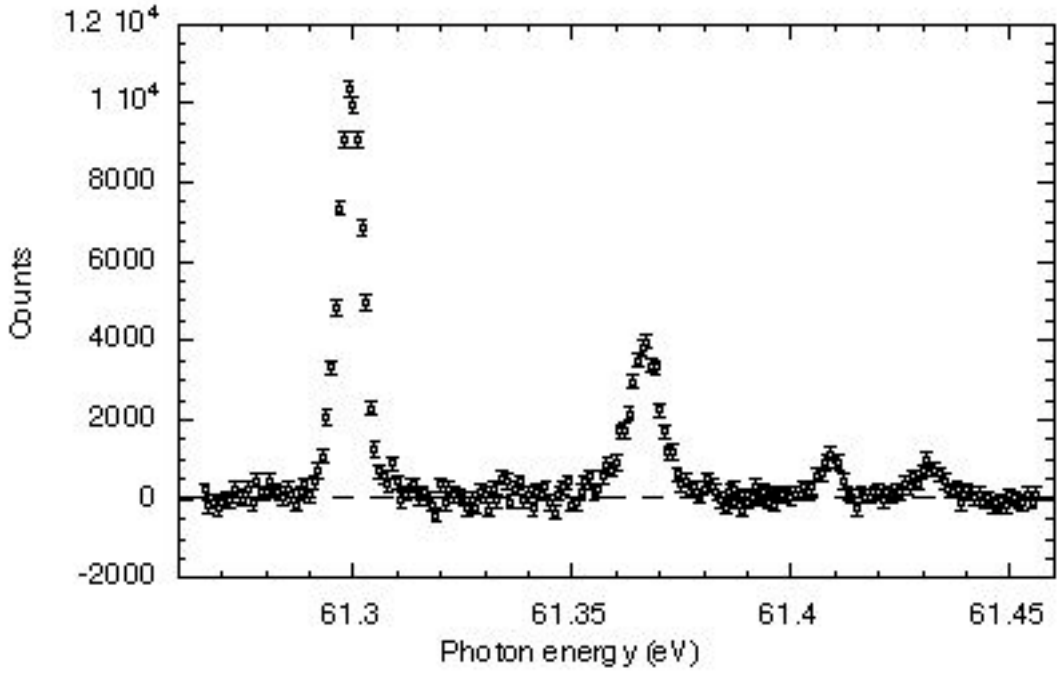

Figure 1: The photoionization spectrum of Mg^+.

RESULTS

For Mg^+ measurements were made over the photon energy range 61-68 eV, and a sample of these is shown in Fig. 1;these are preliminary results which have not been normalised and they are therefore relative. Four lines are evident, where previously one was observed. The lines at 61.30 and 61.37 are to be associated with transitions to the $2p^5 3s3d(^3D)\ ^2P$ levels of Mg^+, and the remaining two lines are probably due to transitions to the $2p^5 3s4s(^1S)$ levels. In Fig. 2 the corresponding region for Al^+ is shown. Rydberg series converging to the $2p^5 3s^2$ level of Al^{2+} at $\sim$92 eV are clearly evident.

Although a straightforward quantum defect analysis has been applied to the data above, the results are far from conclusive because of the large degree of configuration interaction taking place; the assumption of LS coupling may also be invalid. Even the above assignments must remain tentative until theoretical calculations are available; such calculations, using both the Multiconfigurational Hartree-Fock and R-matrix methods, are currently in progress.

ACKNOWLEDGMENTS

We are indebted to Andrew Mei of the LBL workshops, without whose skill in machining ceramic components for the metal vapour oven the experiments described here would not have been possible.

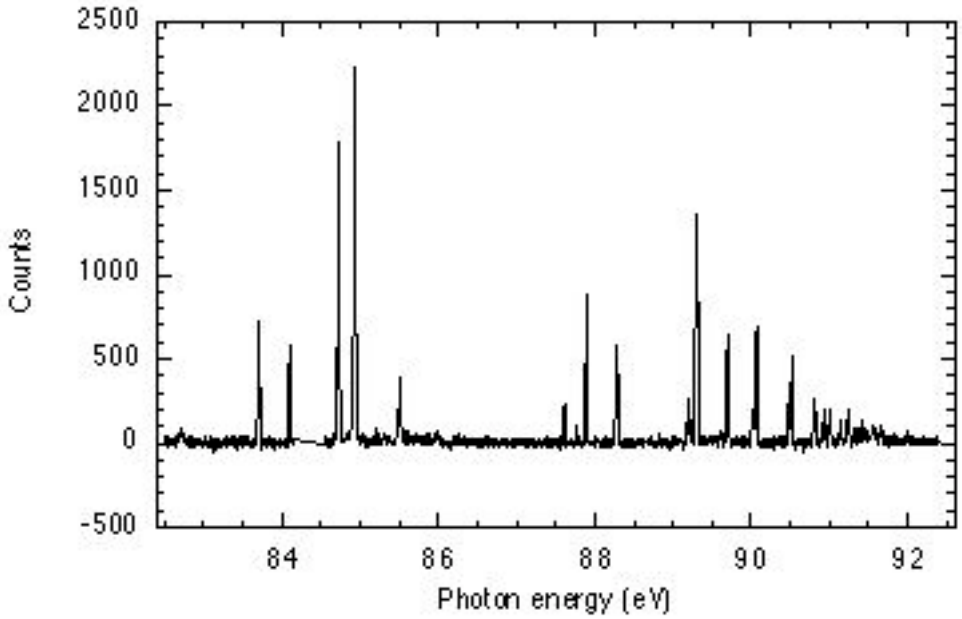

Figure 2: The photoionization spectrum of Al^+.

References

[1] H Kjeldsen, J B West, F Folkmann, H Knudsen and T Andersen T *J. Phys. B: At. Mol. Opt. Phys.* **33** 1403 (2000)

[2] J B West, T Andersen, R L Brooks, F Folkmann, H Kjeldsen and H Knudsen *Phys. Rev.* A **63** 052719 (2001)

[3] B Peart, J G Stevenson and K Dolder *J. Phys. B: At. Mol. Phys.* **6** 146 (1973)

[4] I C Lyon, B Peart, J B West and K Dolder *J. Phys. B: At. Mol. Phys.* **19** 4137 (1986)

[5] A R Covington *et al Phys. Rev. Lett.* **87** 243002 (2001)

This work was supported by the DOE, Contract No. DE-AC03-76SF00098, and in part by a research grant to JBW from the UK Engineering and Physical Sciences Research Council, by the DoE Divisions of Chemical Sciences, Geosciences, Physical Sciences and Materials Sciences, and by the DoE Facilities Initiative. Support was also provided by the Aarhus Center for Atomic Physics, through funding from the Danish National Research Foundation, and by DGAPA-UNAM.

Principal investigator: John B West, CLRC Daresbury Laboratory, Warrington WA4 4AD, United Kingdom. Email: j.b.west@dl.ac.uk.Telephone: +44 (0)1925 603241.

K-Shell Photodetachment of Li^-: Experiment and Theory

J. D. Bozek[1], A.A. Wills[2], G. Turri[1,2], G. Akerman[1], B. Rude[1], H.-L. Zhou[3], S. T. Manson[3], N.D. Gibson[4], C.W. Walter[4], L. VoKy[5], A. Hibbert[6], R.A. Phaneuf[7], S.M. Ferguson[2] and N. Berrah[2]

[1]Lawrence Berkeley National Laboratory, Advanced Light Source, Berkeley, Ca 94720
[2]Western Michigan University, Physics department, Kalamazoo, MI 49008
[3]Department of Physics and Astronomy, Georgia state University, Atlanta, GA 30309
[4]Department of Physics and Astronomy, Denison University, Granville, Ohio 43023
[5]DAMAP, UMR 8588 du CNRS, Observatoire de Paris 92195, Meudon Cedex, France
[6]Queen's University of Belfast, Belfast, BT7 1NN, United Kingdom
[7] University of Nevada, Reno, NV89557

Introduction

Investigation of the dynamics in negative ions provides valuable insights into the general problem of the correlated motion of electrons in many-particle systems, such as heavy atoms, molecules, clusters and solids. Photoexcitation and photodetachment processes of negative ions stand out as an extremely sensitive probe and theoretical test bed for the important effect of electron-electron interactions because of the weak coupling between the photons and the target electrons. In addition, negative ions present a severe theoretical challenge since the independent electron model is inadequate for even a qualitative description of their properties. Finally, studies of the properties of negative ions are needed since their production and destruction strongly affects systems such as dilute plasmas appearing in the outer atmospheres of stars. It has long been thought that electron correlations mainly involve the outer shell electrons of a negative ion, and only outer shell correlations were considered in theoretical calculations. However, new theoretical [1] works including core-valence and core-core effects has recently led to a better agreement with experiments. The present work shows how all the four electrons of Li^- are strongly affected by correlations. Li^-, ground state $1s^22s^2$ (^1S), is one of the simplest negative ions. However, its extended nuclear core, as compared to H^-, has a profound effect on the resonance structure. The lifting of the degeneracy of different l states with the same quantum number n opens up new decay channels. Outer-shell structures in the photodetachment cross section of Li^- have been extensively investigated experimentally [2,3] and they were well explained by theoretical calculations [4,5]. However, up until a very recent calculation [6] no published work in inner-shell photodetachment of negative ions was available other than the inner-shell theoretical work in He^- [7,8]. With the advent of 3rd generation synchrotron light sources with higher flux, brightness and resolution, it is now possible to investigate experimentally inner-shell processes in tenuous negative ion targets.

Experiment and theory

In this work, we report dramatic structure measured and calculated for the K-shell photodetachment of Li^-. This process leads to a core-excited state of Li which decays predominantly to the Li^+ ion. The measurements were performed at ALS Beamline10.0.1, used in tandem with the photon-ion experimental apparatus [9]. Li^- ions were produced using a cesium sputtering source (SNICS II) [10]. The Li^- ion beam was accelerated to 11 KeV, and a flux of 20-150 nA reached the interaction region. The ions were merged collinearly with the counterpropagating photon beam in a 30 cm long energy-tagged interaction region, producing neutral Li atoms and Li^+ ions. Li^+ ions were detected as a function of photon energy, using a photon resolution of 75 meV. The resulting signal was normalized to the primary Li^- ion beam and the incident photon flux. In the case of negative ions, merged experiments are a serious

challenge since the signal is very easily swamped by background noise due to stripping of negative ions with the residual gas (even though the background pressure in the interaction region was ~ 10^{-10} Torr) or with apertures in the ion beamline. In order to correct for the background ionization, the photon beam was chopped at 1 Hz and the photodetachment signal, corresponding to a relative cross section, was determined by subtracting the light-off signal from the light-on signal. The statistical error in the data was decreased by summing multiple sweeps of the photon energy of interest. The photon energies were calibrated separately using known resonance positions for neutral gasses and corrected for the Doppler shift, which amounts to about 108 meV for 60 eV photons. Calculations of the photodetachment of Li^- were performed using the R-matrix methodology which was enhanced to handle negative ions [11] and inner shells [12]. The discrete state input was generated with CIV3 [13]. A total of 29 target states were included in the close-coupling expansion: five $1s^2nl$ states, $n \leq 3$ and $l \leq 2$, and 24 1s2l3l', l=2,3, l'=0,1,2 core-excited states of Li. The cross section for Li^+ production for the Li^- photodetachment was obtained by summing all the cross sections for all of the channels leading to core-excited Li, since Li with a 1s-vacancy decays via Auger process virtually 100% of the time [14].

Results

The measured relative intensity was normalized to the magnitude of the calculated cross section at 62 eV. The calculated spectrum required only a small shift, +0.2 eV, to align to experimental data. It is interesting to note that this energy discrepancy is the same as that found in the case of photoionization of neutral Li [15]. The experimental and theoretical data are reported in Fig.1, where the neutral Li thresholds are reported.

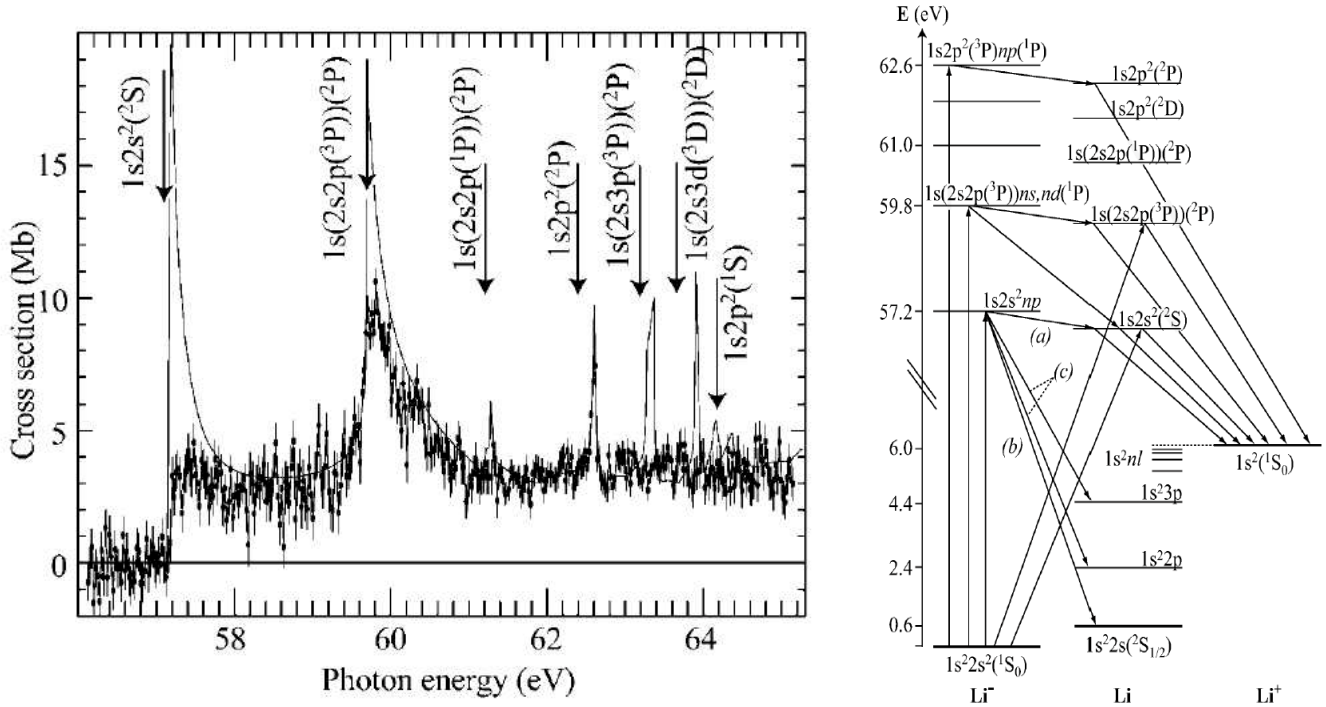

Fig.1 (left) Total double photodetachment cross section of Li^- giving rise to Li^+ in the vicinity of the 1s threshold. The solid curve is the R-matrix calculation and the dots with error bars are the experimental data normalized to the calculation at 62 eV. The arrows indicate the neutral Li thresholds. (right) Schematic energy level diagram (see text for details).

The experimental data clearly show three structures: first a step above the $1s2s^2\ ^2S$ threshold around 57.2 eV; second a shape resonance well defined by its sharp rise and decay tail above the second threshold $1s(2s2p\ ^3P)\ ^2P$; third a narrow resonance above the $1s2p^2\ ^2P$ threshold around 62.6 eV. Agreement between theory and experiment is quite good for the latter two structures, whereas the measured spectrum does not show the theoretically predicted shape resonance structure in the region above the first 1s detachment threshold. Li^+ can be produced in this energy region by autodetachment of the $1s2s^2np\ Li^-$ shape resonance to the core-excited $1s2s^2\ ^2S$ state of Li, which subsequently undergoes Auger decay to the ground state of Li^+, as labeled by process (a) in the energy level diagram of Fig, 1.

A similar process leads to the observed resonance structure above the second 1s threshold at 59.65 eV. In order for the $1s2s^2np\ Li^-$ states to produce Li^+, these states must be at higher energy than the first core-excited state of Li. As illustrated in the energy level diagram of Fig.1, this is the case for the $1s2s^2np$ excitations, which are found to be slightly above the $1s2s^2\ ^2S$ threshold for Li. Note that this situation is quite different from the case of neutral atoms, in the sense that there is not an infinite Rydberg series converging to each threshold. The lack of signal in the positive ion channel suggests that the $1s^2np$, $n>3$ states, omitted in the calculations, may play a significant role, since our results [16] are corroborated by an independent work [17].

It is surprising to find that the experiment was able to resolve and measure the predicted narrow structure above the $1s2p^2\ ^2P$ threshold around 62.6 eV, but not the predicted structures above the $1s(2s3p\ ^3P)^2P$ or $1s(2s3d^3D)^2D$ threshold above 63 eV or the weaker structure above the $1s(2s2p^1P)^2P$ around 61 eV. In the case of this last threshold, it may be that the signal to noise ratio is not sufficient to allow the observation of this weak structure. However the structure at 62.6 eV is expected to be stronger and narrower than the one at 63.2 eV, so at the moment we have no explanation for the discrepancy between experiment and theory in this region.

Conclusion

The first comparison between an experiment and theoretical K-shell study of the photodetachment of Li^- reveals dramatic structure, qualitatively and quantitatively unlike the same process in atomic Li or Li^+ ion. The calculations are able to predict the structures decaying to Li^+ in some cases, whereas the decay cross section is overestimated in the case of $1s(2s2p^3P)^2P$ and $1s2s^2\ ^2S$ thresholds. It is evident to us that although much of the essential physics of the inner-shell photodetachment problem is embodied in the calculation, there is still more to be understood, even in this simplest multishell negative ion.

Funding

DOE, Office of Science, BES, the NFS and NASA

Publication

N. Berrah *et al.*, K-Shell Photodetachment of Li^-: Experiment and Theory, Phys. Rev. Lett. 87, 253002 (2001).

References

[1] T. Andersen *et al.*, J. Phys. Chem. Ref. Data 28, 1511 (1999) and references therein

[2] G. Haeffler *et al.*, Phys. Rev. A 63, 053409 (2001) and references therein

[3] U. Berzinsh *et al.*, Phys. Rev. Lett. 74, 4795 (1995) and references therein

[4] C. Pan *et al.*, J. Phys. B 27, L137 (1994) and references therein

[5] E. Lindroth, Phys. Rev. A 52, 2737 (1995) and references therein

[6] H.-L. Zhou *et al.*, Phys. Rev. Lett. 87, 023001 (2001)

[7] D-S Kim *et al.*, J. Phys. B 30, L1 (1997)

[8] J. Xi and C.F. Fisher, Phys Rev. A 59, 307 (1999)

[9] A.M. Covington *et al.*, Phys. Rev. Lett. 87, 243002 (2001)

[10] R.D. Rathmell and G.A. Norton, Nucl. Instrum. Methods Phys. Res., Sect. B21, 270 (1987)

[11] H.-L. Zhou *et al.*, Phys. Rev. A 64, 012714 (2001)

[12] H.-L. Zhou *et al.*, Phys. Rev. A 59, 462 (1999)

[13] A. Hibbert, Comput. Phys. Commun. 9, 141 (1975)

[14] W. Bambynek *et al.*, Rev. Mod. Phys. 44, 716 (1972)

[15] S. Diehl *et al.*, Phys. Rev. Lett. 84, 1677 (2000)

[16] N. Berrah *et al.*, Phys. Rev. Lett. 87, 253002 (2001)

[17] B.H. Kjeldsen *et al.*, J. Phys. B 34, L353 (2001)

Principal investigator: Nora Berrah, Physics Department, Western Michigan University, Kalamazoo, MI 49008.
Telephone: (1) 616-387-4955. Fax: (1) 616-387-4939. Email: berrah@wmich.edu.

K-shell photoexcitation of carbon ions: lifetime of a K-shell vacancy

A. S. Schlachter[1], M. M. Sant'Anna[1,2], A. M. Covington[3], A. Aguilar[3], M. F. Gharaibeh[3], G. Hinojosa[4], R. A. Phaneuf[3], I. Alvarez[4], C. Cisneros[4], A. Müller[5], B. M. McLaughlin[6]
[1]Advanced Light Source, Ernest Orlando Lawrence Berkeley National Laboratory, University of California, Berkeley, California 94720, USA
[2]Pontificia Universidade Catolica do Rio de Janeiro, Rio de Janeiro 22452-970, Brazil
[3]Department of Physics, MS 220, University of Nevada, Reno, Nevada 89557-0058, USA
[4]Centro de Ciencias Fisicas, Universidad Nacional Autonoma de Mexico, Apartado Postal 6-96, Cuernavaca 62131, Mexico
[5]Institut für Kernphysik, Universität Giessen, D-35392, Giessen, Germany
[6]School of Mathematics and Physics, Queen's University of Belfast, Belfast BT71NN, UK

INTRODUCTION

Carbon is ubiquitous in nature and is the building block of life. The carbon atom in its various states of ionization has a small number of electrons, and is thus amenable to theoretical study. Given the importance of the carbon atom, it is surprising that there are few detailed measurements of inner-shell photoionization or photoexcitation processes, and that the lifetime of a K-shell vacancy in a free carbon atom is not experimentally known. The major difficulty is that free carbon atoms cannot readily be produced. In the present investigation we have measured photoexcitation of a C^+ ion rather than photoionization of a neutral carbon atom, producing the same state of C^+ as would be produced by direct photoionization of a neutral carbon atom. Photoexcitation of C^{2+} and C^{3+} has also been studied, both experimentally and theoretically.

LIFETIME OF A K-SHELL VACANCY

The lifetime of a K-shell vacancy in a free carbon ion (C^+) has been measured as part of a study of photoexcitation of K-shell electrons in carbon ions. The lifetime is determined by measuring the energy width of the resonance created by photoexcitation of a K-shell electron in the C^+ ion: the innermost 1s electron is promoted to the 2p shell, resulting in production of the $1s2s^22p^2\ ^{2,4}P$, ^2S, ^2D autoionizing states. The excited state of the C^+ ion produced in this experiment is identical to that produced by direct K-shell photoionization of the neutral carbon atom. Knowledge of such lifetimes is important for comparative studies of the autoionization widths for a K-shell vacancy in hydrocarbons and other carbon-containing molecules, where the molecular properties are known to affect the charge distribution and therefore the core-hole lifetimes and autoionization rates.

PHOTON-ION MERGED-BEAMS EXPERIMENT

A photon beam on beamline 10 is merged with a well-collimated energy- and charge-state-selected ion beam from a small accelerator [1]. The ion beam is charge-state analyzed after the interaction region: the primary ion beam is collected by a Faraday cup, while ions whose charge state has increased are detected and counted. The photon beam is time modulated to subtract ions which have changed their charge state in collision with background gas. All experimental parameters can be measured for determination of absolute cross sections; however, only relative cross sections have been measured in the present experiment.

RESULTS: ELECTRON SCREENING

Photon energy was scanned over the energy range where resonances are predicted by theory. Relative cross sections for photoexcitation of an admixture of ground-state and metastable C^+, C^{2+}, and C^{3+} beams are presented in Fig. 1. The insets show small peaks which would not be visible on the scale of the larger resonances. Experimental energies have been corrected for the Doppler-shift of the moving ions, and the energy scale has been determined relative to photoabsorption in CO. The large energy shift in the resonances with increasing charge state of the incident ion seen in Fig 1 is due to electron screening: there are fewer electrons on an ion in a higher charge state to pass between the nucleus and the K-shell electrons which reduce the nuclear charge felt by the K-shell electrons. Theoretical calculations using state-of-the-art techniques are in good agreement with the measurements. This comparison is valuable for benchmarking theory and for interpreting x-ray satellite data.

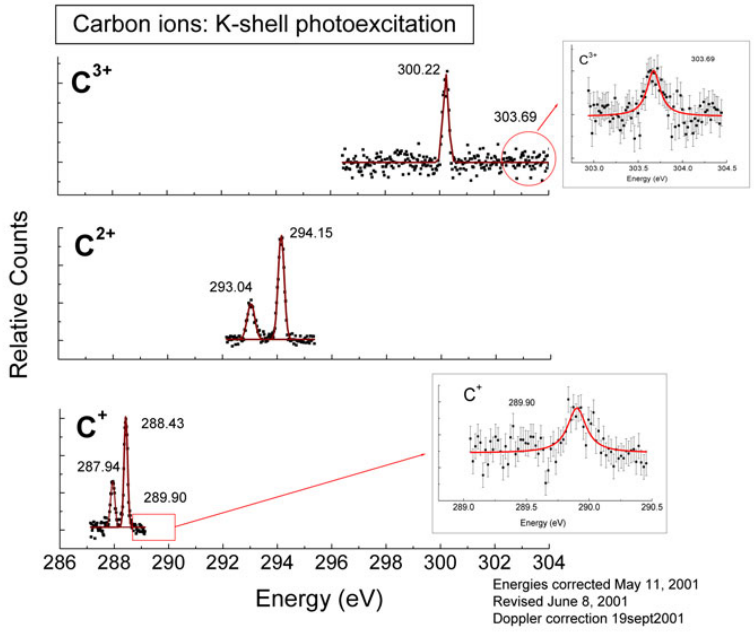

Figure 1. Experimental K-shell photoexcitation cross sections for C^+, C^{2+}, and C^{3+} ions. Relative cross sections are shown, for an admixture of ground-state and excited-state ions.

Natural linewidth can be measured in some cases by varying the spectral resolution of the incident photon beam, accomplished by changing the width of the entrance and exit slits of the monochromator. Data have been obtained for photoexcitation of C^+ ions with three different nominal spectral resolutions: 200 meV, 100 meV, and 50 meV. The resonance peaks were fit with a Voigt profile, which is a convolution of a Gaussian and a Lorentzian profile. The Gaussian width is instrumental, while the Lorentzian width is the natural lifetime width of the resonance. The fit was done on the two larger peaks, constrained to have the same Gaussian width for the same nominal resolving power. Results are shown in Fig. 2. The same value of lifetime linewidth was obtained for all three nominal spectral resolution values, providing confidence in the validity of the fitting process. The result is a width of 54 +/- 4 meV for the higher-energy peak and 102 +/- 10 meV for the lower-energy peak. It is interesting to note that the actual spectral resolution determined by the Gaussian width is better than the nominal resolution for relatively wide slits, but approaches the nominal width for the narrowest slits. This is because the undulator beam does not fill the entrance slit of the monochromator except for narrow settings of the entrance slit—which is the case for high spectral resolution.

The linewidth of a carbon-atom K-shell vacancy in a molecule is known to be greater than the theoretical linewidth of a free carbon atom due to molecular properties, e.g., charge distribution in the molecule. Coville and Thomas [2] and Carroll et al [3] list both theoretical and experimental values for a wide variety of carbon-containing molecules. A notable absence is that of an experimental value for a free carbon atom. (N.b., a carbon atom with a K-shell vacancy is, of course, a C^+ ion.) Two features are apparent from their work: the significant disagreement between experiment and theory; and the linewidth of a carbon K vacancy in all molecular species studied is significantly greater than the theoretical linewidth of a free carbon atom. The theoretical linewidth of a K-shell vacancy produced in a free carbon atom (thus in a C^+ ion) is 56 meV [2]. However, until now there have been no measurements of this linewidth. Furthermore, measurements of linewidths by photoionization of a molecular species are often complicated by post-collision interactions and other factors. The experimental method reported here, the production of the K-vacancy state of an atom by photoexcitation of the ion, does not have PCI, as there are no slow electrons to influence the lineshape. The lifetime of a K-shell vacancy is shorter in all molecules (the linewidth is greater) than in an isolated carbon atom. The present results are therefore significant in understanding vacancy-filling mechanisms in molecules. The measured lifetime agrees well with theory.

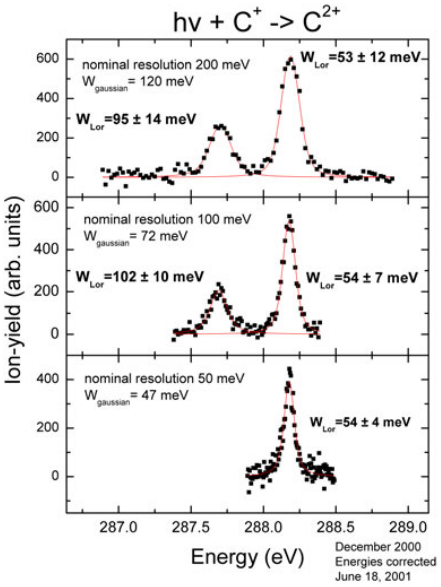

Figure 2. Experimental relative cross section for photoexcitation of C^+ ions, for three different values of nominal spectral resolution. The Gaussian width is the experimental resolution, the Lorentzian width is the lifetime width of each peak.

REFERENCES

[1] Covington et al, Phys. Rev. Letters **87**, 243002 (2001).
[2] Coville and Thomas, Phys. Rev. A **43**, 6053 (1991).
[3] Carroll et al, Phys. Rev. A **59**, 3386 (1999).

This work was supported by the Director, Office of Energy Research, Office of Basic Energy Sciences, Materials Science Division, of the U.S. Department of Energy under Contract No. DE-AC03-76SF00098, and the Division of Chemical Sciences, Geosciences and Biosciences

Principal investigator: R. A. Phaneuf, Department of Physics, University of Nevada, Reno NV 89557-0058. Email: phaneuf@physics.unr.edu. Telephone: 775 784-6818.

MIRRORING DOUBLY EXCITED RESONANCES IN NEON

S.E. Canton[1,2], A.A. Wills[2], T. W. Gorczyca[2], M. Wiedenhoeft[2],
E. Sokell[3], J.D. Bozek[1], G. Turri[1,2],Ximao Feng[2], and N. Berrah[2]
[1] Lawrence Berkeley National Laboratory, Advanced Light Source, University of California, Berkeley CA 94720.
[2] Department of Physics, Western Michigan University, Kalamazoo MI 49008.
[3] Department of Experimental Physics, University College Dublin, Ireland.

INTRODUCTION

The combination of high photon resolution and differential photoelectron spectroscopy techniques has allowed the discovery of new spectral features in the low-energy photoionization spectrum of neon. These resonances observed in the $2p^{-1}{}_{1/2,3/2}$ partial cross sections are attributed to LS forbidden doubly excited states with mirroring profiles [1]. The present results highlight the need for including relativistic interactions in the theoretical description of the photoexcitation process even for light systems.

EXPERIMENT

The experiment was performed on beamline 10.0.1 at the ALS. The apparatus consisted in two time of flight analyzers at 54.7^0 and 0^0 with respect to the electric field axis housed in a rotatable. The data was collected and displayed using a two dimensional acquisition technique consisting of recording data at closely spaced photon energies from which constant ionic spectra (CIS) were extracted as shown in Fig.1 to Fig.4. When the two photoelectron peaks corresponding to $2p^{-1}{}_{1/2,3/2}$ spaced by 97 meV are separated, the overall resolution of the CIS depends solely on the photon bandwidth. The spectral resolution was about 3 meV, close to the 10,000 resolving power obtainable at this beamline.

RESULTS

The present experiment follows up on previous work related to mirroring effects in Argon [2,3]. It gives the most detailed account of the resonant structure below the second ionization potential in neon up to date. In addition to the singly excited Rydberg series and the pronounced $2s^22p^4(^3P)3s(^2P)3p(^1P)$ excited state ,many new weak doubly excited states were observed. The strength of the experimental technique is fully demonstrated as most of the features can only be detected through the extraction of the corresponding branching ratio and at specific angles. Considering their energy position, they have been assigned with an LS forbidden triplet symmetry. For some of them, this is clearly confirmed by their mirroring profiles in the partial cross sections as shown in Fig.1 and Fig.2. The breakdown of LS coupling is further demonstrated by the branching ratio differing from the statistical value 2 by 10% throughout the whole spectral range. A complete calculation of the photoionization spectrum reproducing these highly correlated and spin-orbit induced resonances is still beyond the capabilities of available codes. However, it is hoped that this work will provide useful guidelines for further studies.

REFERENCES

[1] C.N. Liu, A.F Starace, Phys. Rev. A **59** R1731 (1999).
[2] S.E. Canton-Rogan, A.A. Wills, T.W. Gorczyca, M. Wiedenhoeft, O. Nayandin, C.N. Liu, and N. Berrah, Phys. Rev. Lett. **85**, 3113 (2000).
[3] C.D. Caldwell, S.B. Whitfield, and M.O. Krause, Mol. Phys, **98,** 1075 (2000).

This work was funded by the Department of Energy, Office of Science, Basic Energy Sciences, Chemical and Material Science Division, under the contract No. DE-FG02-92ER14299.

Principal investigator: Nora Berrah, Physics Dept., Western Michigan University, 616-387-4955, berrah@wmich.edu.

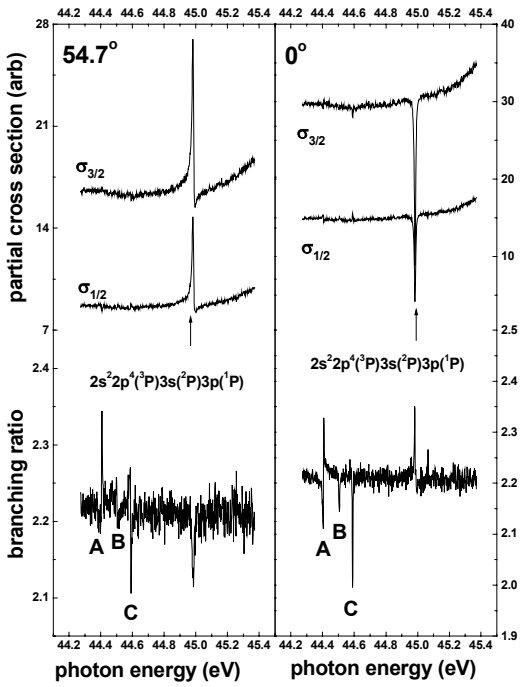

Fig.1: Partial differential cross sections meas-ured at the magic angle 54.7˚ and 0˚ with cor-esponding branching ratio in the vicinity of the first doubly excited state $2s^22p^4(^3P)3s(^2P)3p(^1P)$. Labels A, B, C indicate the position of the new doubly excited resonances.

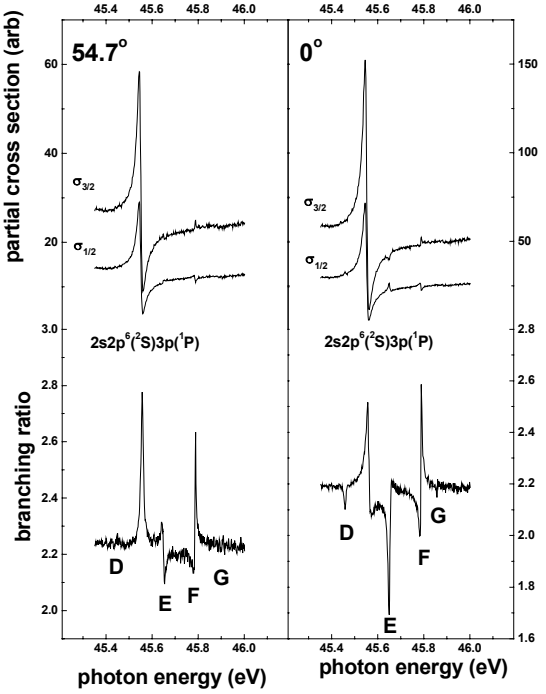

Fig.2: Partial differential cross sections measured at the magic angle 54.7˚ and 0˚ with corresponding branching ratio in the vicinity of the first singly excited state $2s2p^63p(^1P)$. Labels D, E, F, G indicate the position of the new doubly excited resonances.

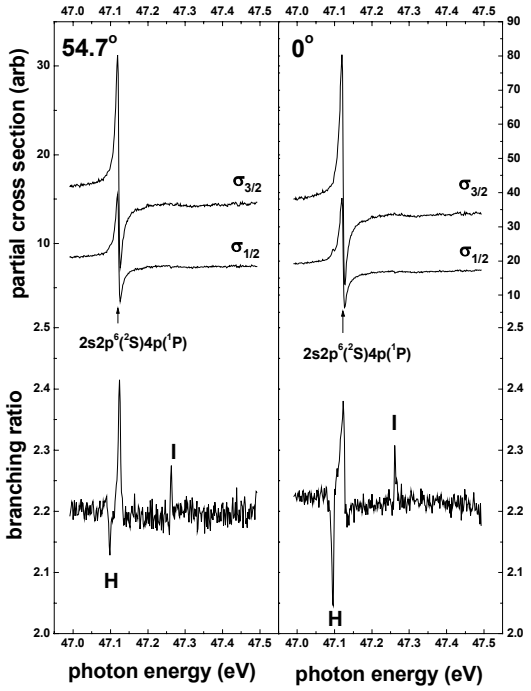

Fig.3: Partial differential cross sections measured at the magic angle 54.7˚ and 0˚ with corresponding branching ratio in the vicinity of the second singly excited state $2s2p^64p(^1P)$. Labels H, I indicate the position of the new doubly excited resonances.

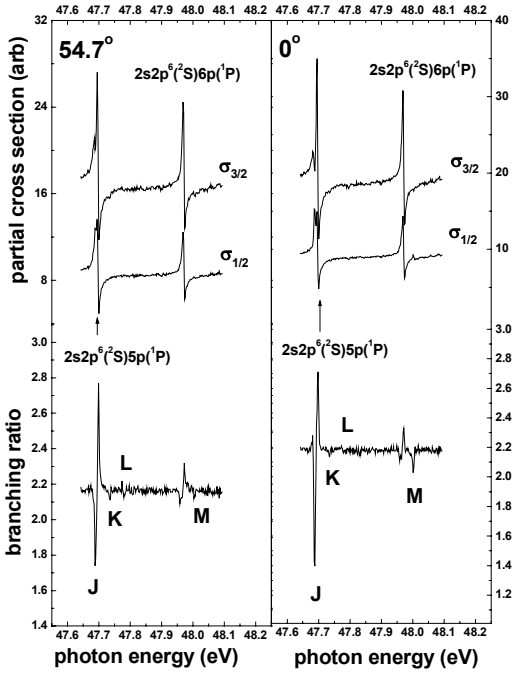

Fig.4: Partial differential cross sections measured at the magic angle 54.7˚ and 0˚ with corresponding branching ratio in the vicinity of the third and fourth singly excited state $2s2p^65p(^1P)$ and $2s2p^66p(^1P)$. Labels J, K, L, M indicate the position of the new doubly excited resonances.

Photoionization of C^{2+} ions

A. Müller[1], R. A. Phaneuf[2], A. Aguilar[2], M. F. Gharaibeh[2], A. S. Schlachter[3], I. Alvarez[4], C. Cisneros[4], G. Hinojosa[4] and B. M. McLaughlin[5]

[1]Institut für Kernphysik, Universität Giessen, D-35392 Giessen, Germany
[2]Department of Physics, MS 220, University of Nevada, Reno, NV 89557-0058, USA
[3]ALS, Lawrence Berkeley National Laboratory, Berkeley, CA 94720, USA
[4]Centro de Ciencias Físicas, UNAM, Apartado Postal 6-96, Cuernavaca 62131, México
[5]School of Math. and Physics, Queen's University of Belfast, Belfast BT7 1NN, UK

Photo*absorption* in the interstellar medium modifies the radiation spectrum of distant objects in the universe and thus complicates the interpretation of observations of such objects. Photo*ionization* of ions is an important mechanism for the production of highly charged ions in astrophysical plasmas exposed to hot sources of radiation. Ionization in such plasmas is usually balanced by low-energy electron-ion recombination. Because of their applied importance photon-ion and electron-ion collision processes have received long-standing interest by the plasma and astrophysics communities [1].

The pair of C^{2+} and C^{3+} ions is of particular interest for the understanding of astrophysical and man-made plasmas. Photoionization (PI) of C^{2+}

$$h\nu + C^{2+} \rightarrow C^{3+} + e \tag{1}$$

is the time-reversed (photo-)recombination (PR)

$$C^{3+} + e \rightarrow h\nu + C^{2+}. \tag{2}$$

Both reactions can proceed directly or in a multi-step fashion involving intermediate production of multiply excited autoionizing states. The indirect (resonant) PR channel is also called dielectronic recombination (DR). The principle of detailed balance, based on time-reversal symmetry, relates the cross sections of PI and PR on a state-to-state basis. Measuring one or the other of the two cross sections provides information about the time-reversed process. High resolution PR experiments with C^{3+} ions have been performed previously at heavy-ion storage rings [2, 3].

Here, we report on the first high-resolution PI experiments carried out with multiply charged ions at the Advanced Light Source (ALS). Our measurements are compared with state of the art theoretical calculations performed within the semi-relativistic Breit-Pauli R-matrix method. Absolute cross sections were determined at a number of selected energies by employing a suitable photon-ion merged beams technique. In addition, relative energy-scan measurements were carried out to cover a wide energy range in narrow energy

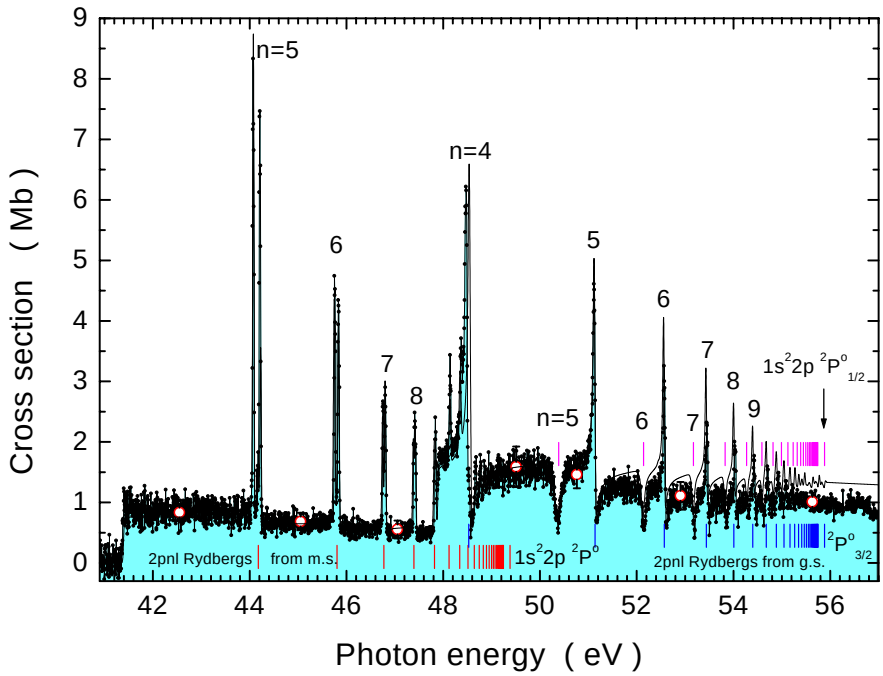

Figure 1: Measured and calculated cross sections for PI of C^{2+} ions. The energy-scan measurement is indicated by small dots connected by straight lines the area under which is shaded. The scan data were normalized to separate absolute PI cross section measurements (open circles with total error bars). The solid line represents the weighted sum of the R-matrix results assuming 60% of ground state (g.s.) ions in the primary beam, 30% in the $^3P_0$ and 5% each in the $^3P_1$ and $^3P_2$ metastable (m.s.) states. The theoretical result is almost indistinguishable from the measurements below 51 eV. The main Rydberg series of intermediate autoionizing states are indicated by vertical bars.

steps. The relative data were then normalized to the absolute cross sections. The C^{2+} target ions were produced with an all-permanent-magnet electron cyclotron resonance (ECR) ion source.

Fig. 1 shows an overview of the results obtained from the present experiment and theoretical calculations. The open circles represent the absolute cross sections. Total experimental uncertainties of these data are indicated by error bars. The normalized scan data are visualized by the shaded area. Theory is represented by a solid line obtained after convoluting the calculated results with a gaussian of 30 meV full width at half maximum. Excellent agreement between theory and experiment is obtained by assuming that the parent C^{2+} ion beam consisted of 60 % ground state ions and 40 % metastable ions (with 30% in the $^3P_0$ and 5% each in the $^3P_1$ and $^3P_2$ states). Almost perfect agreement of theoretical and experimental level energies is found.

Qualitatively, the PR experiments [3] show the same features as the PI data of Fig 1. The cross section is also dominated by ($2pnl$) Rydberg resonances. Near threshold, i.e.

just above the (PI) ionization limit of C^{2+} and just above zero electron energy in the e + C^{3+} (PR) measurement the energy resolution is comparable in both the PI and the PR experiments. The resolution is sufficient to determine the natural line width of some of the states involved. Also the energy scales of both experiments agree very well within uncertainties of the order of less than 15 meV. However, the time-reversed PR measurement produces cross sections which are roughly two orders of magnitude above the present PI results. This apparent discrepancy may be understood in terms of how the data are obtained in the different experiments and how the related cross sections are defined. The PI experiment was carried out with a mixed beam of ground state and metastable ions. PI including the resonance contributions can populate the ground state of C^{3+} and at energies above 49.380 eV (for the metastable beam component) and 55.883 eV (for the ground state component) also the first excited states of C^{3+} which thus contribute to the measured cross section. In the storage ring PR experiments, however, only ground state C^{3+} ions were investigated. So there are contributions in the measured PI cross section that are not included in the PR data. The opposite is also true. Due to the relaxed selection rules for electron-ion collisions PR can populate many more autoionizing resonances than photoexcitation, which is essentially restricted to electric dipole transitions. In addition the PR resonances can decay to excited C^{2+} states which were not accessible to the PI measurements. In the light of this discussion it becomes clear that detailed balance has to be applied with care; it is valid only on a state-to-state basis. Consequently, PI and PR experiments nicely complement rather than duplicate each other providing additional information that would not be accessible by just one of the measurements. Branching ratios for different decay paths (or excitation pathways in opposite direction) of multiply excited states can be quantified by the comparisons. For example, the relative probability of the two-electron one-photon de-excitation of the $C^{2+}(1s^2 2p4d\,^1P)$ resonance could be inferred to be about 7.9 %.

References

[1] M. J. Seaton, Y. Yu, D. Mihalas and A. K. Pradhan, Mon. Not. R. Astron. Soc. **266**, 805 (1994).

[2] S. Mannervik, D. deWitt, L. Engström, J. Lidberg, E. Lindroth, R. Schuch, W. Zong, Phys. Rev. Lett. **81**, 313 (1998).

[3] S. Schippers, A. Müller, G. Gwinner, J. Linkemann, A. A. Saghiri, A. Wolf, Astrophys. J. **555**, 1027 (2001).

This work is supported by NATO Collaborative Linkeage Grant PST.CLG.976362, Deutsche Forschungsgemeinschaft (DFG), the Department of Energy , Office of Basic Energy Sciences, by CONACyT and DGAPA (Mexico), NSF (USA), and by EPSRC (UK).

Principal investigator: Alfred Müller, Institut für Kernphysik, Strahlenzentrum der Justus-Liebig-Universität Giessen, D-35392 Giessen, Germany. Email: Alfred.Mueller@strz.uni-giessen.de. Telephone: xx49 641 99 15200

Photoionization of doubly charged scandium ions

S. Schippers[1], A. Müller[1], S. Ricz[2], M. E. Bannister[3], G. H. Dunn[4], J. Bozek[5], A. S. Schlachter[5], G. Hinojosa[6], C. Cisneros[6], A. Aguilar[7], A. Covington[7], M. Gharaibeh[7], and R. A. Phaneuf[7]

[1]Institut für Kernphysik, Justus-Liebig-Universität, 35392 Giessen, Germany
[2]Institute of Nuclear Research (ATOMKI), H-4001 Debrecen, Hungary
[3]Physics Division, Oak Ridge National Laboratory, Oak Ridge, TN 37831, USA
[4]JILA, University of Colorado, Boulder, CO 80309-0440, USA
[5]Advanced Light Source, Lawrence Berkeley Laboratory, Berkeley, CA, USA
[6]Centro de Ciencas Fisicas, UNAM, Cuernavaca, Mexico
[7]Department of Physics, University of Nevada, Reno, NV 89557, USA

INTRODUCTION

Considering the fact that the ground state configuration of both neutral potassium and singly charged calcium is [Ar]4s, doubly charged scandium with its [Ar]3d ground state configuration is the simplest atomic system with an open 3d shell. It is even simpler than neutral scandium which in addition to the 3d electron has a closed $4s^2$ shell outside the argon core. Therefore photoionization (PI) of Sc^{2+} is fundamentally interesting, especially in view of the severe discrepancies between experimental [1] and theoretical [2] PI cross sections for neutral scandium in the region of $3p \rightarrow 3d$ excitations. For these excitations PI of Sc^{2+} can be represented as

$$\begin{array}{rcl} h\nu + Sc^{2+}(3s^2 3p^6 3d) & \rightarrow & Sc^{2+}(3s^2 3p^5 3d^2) \\ & \searrow & \downarrow \\ & & Sc^{3+}(3s^2 3p^6) + e^-. \end{array} \qquad (1)$$

Here the vertical arrow represents the intermediate doubly excited $3p^5 3d^2$ states decaying predominantly by autoionization via Super-Coster-Kronig transitions (vertical arrow), and the diagonal arrow represents the direct 3d PI channel. It is also possible to study the time reverse of Eq. 1, i. e. the photorecombination (PR) of a $Sc^{3+}(3p^6)$ ion with a free electron (e^-). Theoretically, on a state-to-state level, PI and PR cross sections are linked via the principle of detailed balance. It is evident that the study of both processes yields complementary information about the doubly excited intermediate states involved. Results of Sc^{3+} PR measurements, that have been conducted at the heavy-ion storage ring TSR of the Max-Planck-Institut für Kernphysik in Heidelberg, Germany, are already published [3]. Here, we report on first PI results obtained in August 2001 at the photon-ion research facility located at the ALS undulator beamline 10.0.1.

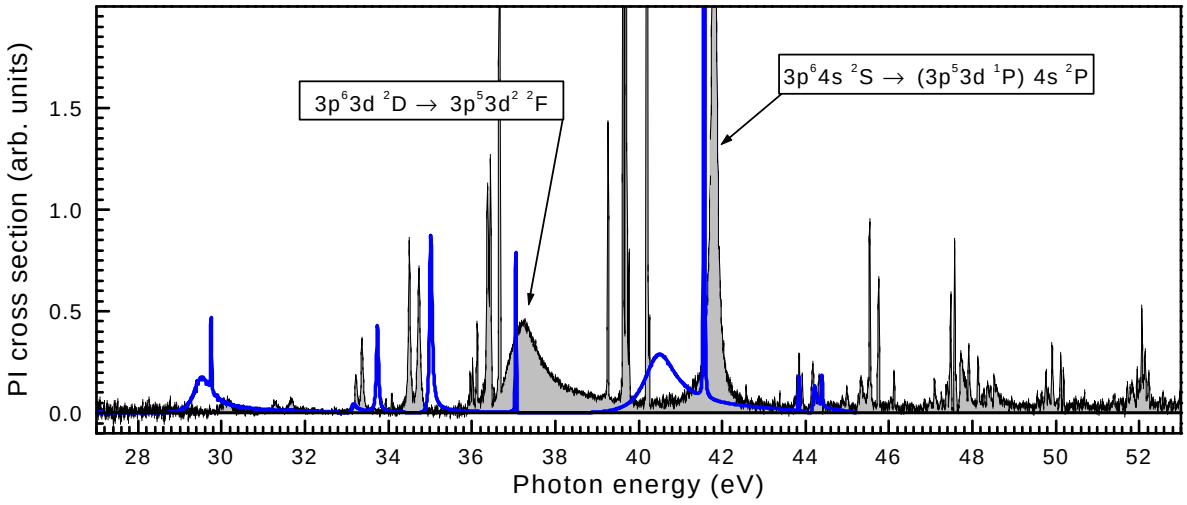

Figure 1: Part of the experimental spectrum (shaded curve) showing prominent resonances due to the excitation of the $3p^6 3d$ ground state and of the $3p^6 4s$ metastable state. The thick full line is the theoretical result of Altun and Manson [2].

EXPERIMENTAL PROCEDURE AND EXPERIMENTAL RESULTS

For the production of the Sc^{2+} ion beam, pieces of metallic scandium were vaporized inside an oven electrically heated to elevated temperatures. The Sc^{2+} ion beam was generated by ionizing the scandium atomic vapor by electron bombardment inside a compact electron cyclotron resonance (ECR) source. After having traveled through a bending dipole magnet serving for selecting the desired ratio of charge to mass, the ion beam was centered onto the counterpropagating monochromatized photon beam by applying appropriate voltages to several electrostatic ion beam steering devices. Electrical ion currents of up to 11 nA were available in the experiment. Behind the interaction zone the ion beam was deflected out of the photon beam direction by a second dipole magnet that also separates the ionized Sc^{3+} product ions from the Sc^{2+} parent ions. The Sc^{3+} ions were counted with nearly 100% efficiency with a single particle detector. From the measured Sc^{3+} count rate the PI cross section is readily derived by normalization on both photon flux and ion current.

The experimental photon energy range 23–68 eV encompasses the direct 3d and 3p photoionization thresholds. The experimental photo-ion spectrum is dominated by autoionizing resonances due to 3p excitations predominantly decaying via Coster-Kronig and Super-Coster-Kronig transitions (Fig. 1). The identification of the resonances is difficult. Only the most prominent resonance features can be identified with the aid of atomic structure calculations. The accurate calculation of resonance energies, widths and strengths for atomic systems with open 3d shells is a challenging task. The highly correlated nature especially of the doubly excited $3p^5 3d^2$ states requires large basis set expansions. Nevertheless, calculated resonance positions deviate by up to 3 eV from the measured resonance energies (Fig. 1).

Figure 2 shows resonances occuring in the energy range 36.62-36.72 eV. The exper-

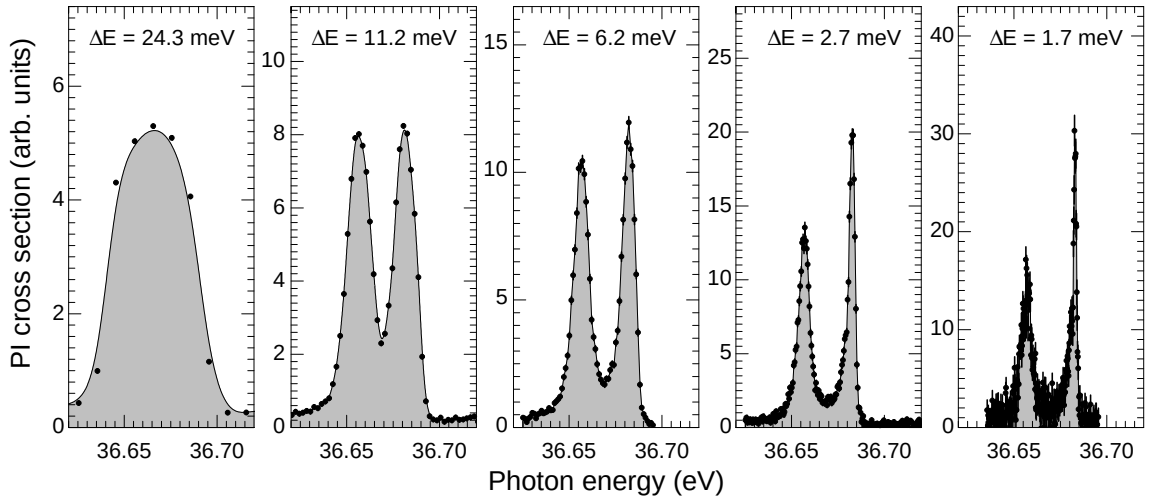

Figure 2: Influence of the experimental resolution on the measured photoionization cross section for a group of 3 resonances located around 36.67 eV.

imental photon energy spread was adjusted in a range of approximately 24 meV down to 1.7 meV by changing the width of the exit slit of the monochromator. At the highest resolution three individual resonances become visible. Likewise individual resonances located around $E \approx 40.2$ eV have been measured with an instrumental energy spread ΔE as low as 1.16 meV corresponding to a resolving power of $E/(\Delta E) \approx 35\,000$.

One complication with multiply charged ion beams extracted from an ECR ion source is the existence of a usually unknown amount of metastable ions in the beam. In the measured PI spectrum of Sc^{2+} (Fig. 1) we have identified resonances due to PI of the $Sc^{2+}(3p^6 3d\,^2D_{3/2})$ ground state as well as resonances due to PI of the $Sc^{2+}(3p^6 3d\,^2D_{5/2})$ and $Sc^{2+}(3p^6 4s\,^2S_{1/2})$ metastable states. A novel possibility to extract the fractions of metastable ions is provided by the comparison of the measured PI cross sections with the experimental PR cross sections of Schippers et al. [3] via detailed balance. The work is still in progress.

References

[1] S. B. Whitfield, K. Kehoe, R. Wehlitz, M. O. Krause, and C. D. Caldwell, Phys. Rev. A **64**, 022701 (2001).

[2] Z. Altun and T. Manson, J. Phys. B **32**, L255 (1999); Phys. Rev. A **59**, 3576 (1999).

[3] S. Schippers, S. Kieslich, A. Müller, G. Gwinner, M. Schnell, A. Wolf, M. Bannister, A. Covington, and L. B. Zhao, Phys. Rev. A (2002), in print.

This work was supported by the NATO Collaborative Research Grants CRG-950911 and CLG-976362.

Principal investigator: Alfred Müller, Institut für Kernphysik, Justus-Liebig-Universität, 35392 Giessen, Germany, Email: Alfred.Müller@strz.uni-giessen.de. Telephone: +49-641-99-15200.

Photoionization of Ne^+: an absolute benchmark for theory

A. M. Covington[1], A. Aguilar[1], I. Álvarez[2], J. D. Bozek, C. Cisneros[2], I. R. Covington[1], I. Dominguez[3], M. F. Gharaibeh[1], G. Hinojosa[1], B. M. McLaughlin[4], M. M. Sant'Anna[3], A. S. Schlachter[3], C. A. Shirley[1] and R. A. Phaneuf

[1]Department of Physics, University of Nevada, Reno, NV 89557-0058, USA
[2]Centro de Ciencias Físicas, Universidad Nacional Autonóma de México, Cuernavaca 62131, México
[3]Advanced Light Source, Lawrence Berkeley National Laboratory, Berkeley, CA 94720, USA
[4]School of Mathematics and Physics, Queens University, Belfast BT7 1NN, U.K.

The photoionization of ions is a fundamental process of importance in many high-temperature plasma environments, such as those occurring in stars and nebulae, as well as in inertial-confinement fusion experiments. Quantitative measurements of photoionization of ions provide precision data on ionic structure, and guidance to the development of theoretical models of multi-electron interactions. In addition, the opacity databases [1, 2] that are critical to the modeling and diagnostics of hot, dense plasmas consist almost entirely of untested coupled-state theoretical calculations based on the R-matrix method. High-resolution absolute photoionization cross-section measurements are therefore needed to benchmark these theoretical methods. Being the sixth-most abundant element in the universe, neon is significant in astrophysics, and therefore Ne^+ was selected for absolute measurements of photoionization cross sections to benchmark a state-of-the-art Breit-Pauli R-matrix theoretical calculation.

The experiments were performed on ALS beamline 10.0.1.2 using the ion-photon-beam (IPB) research endstation [3]. An energy-selected photon beam was merged over a path length of 29 cm with a highly collimated 6 keV Ne^+ beam produced in the hot-filament discharge ion source of the Cuernavaca ion gun apparatus. Two-dimensional intensity distributions of both beams were measured by rotating-wire beam profile monitors installed just upstream and downstream of the interaction region, and by a translating-slit scanner in the middle of the region. A downstream analyzing magnet separated the Ne^{2+} products from the parent Ne^+ beam. A spherical electrostatic deflector directed the Ne^{2+} products onto a biased stainless-steel plate, from which secondary electrons were detected by a microsphere-plate electron multiplier and counted. The absolute efficiency of the photoion detector (0.210 ± 0.005) was determined by measuring the photoion current with an averaging sub-femtoampere meter and comparing it to the measured count rate. The photon beam was mechanically chopped at 0.5 Hz to separate photoions from Ne^{2+} ions produced by stripping collisions of Ne^+ with residual gas in the ultra-high vacuum system. The photon energy and resolution were selected by a precision curved-grating monochromator. The undulator gap was set to maximize the photon intensity at each selected energy. The photon flux was recorded by a calibrated silicon X-ray photodiode, and was typically $2\text{-}3 \times 10^{13}$ photons/second at an energy of 45 eV and a bandwidth of 22 meV.

The absolute photoionization cross-section measurements taken at an energy resolution of 22 meV are compared in Figure 1 with the results of the *ab initio* Breit-Pauli R-matrix theoretical calculation. Two distinct threshold steps are evident at 40.866 eV and 40.963 eV, corresponding to non-resonant photoionization from the $^2P_{1/2}$ metastable state and the $^2P_{3/2}$ ground state, respectively. The calculation represents a sum of the cross sections for photoionization from the ground and metastable states, weighted by their statistical

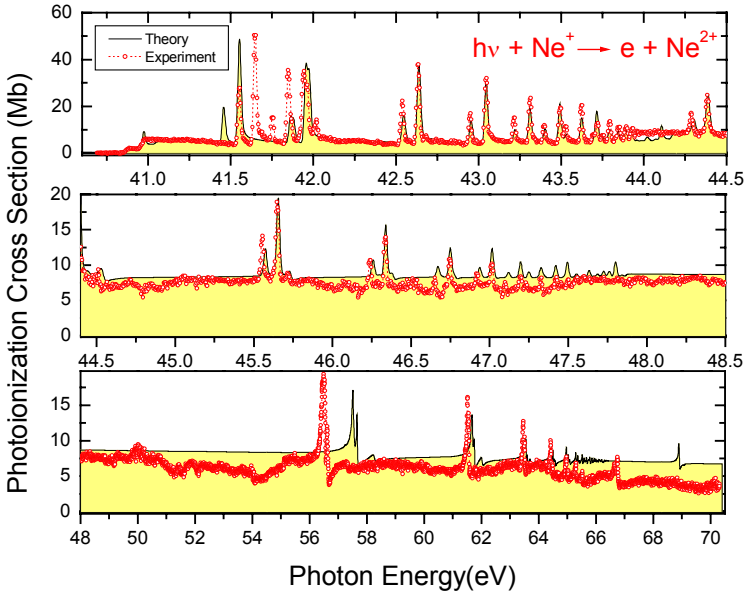

Figure 1. Comparison of absolute measurements (open circles connected by dashed lines) and Breit-Pauli R-matrix theory of McLaughlin (solid curve with shading) for photoionization of Ne^+. The theory has beeen convoluted with a Gaussian of 22 meV FWHM to simulate the bandwidth of the experiment.

weights (2/3 and 1/3, respectively). The calculated non-resonant cross section is almost indistinguishable from the absolute measurement in the energy range 41-44 eV, but diverges from the experiment at higher energies. The origin of the broad structures in the measurements above 44 eV may be interleaved series of $2s2p^4(^1S)ns\ ^2S$ window resonances similar to, but broader than, those observed by Caldwell et al [4] in photoionization of fluorine, which is isoelectronic with Ne^+. It is noteworthy that the predicted energy of the lowest-n resonance differs from experiment by about 100 meV, whereas most of the higher-n resonance energies are in agreement within 10 meV or better. The predicted energy of the $2s2p^5(^3P_2)3p$ resonance feature lies above the measured value of 56.49 eV by more than 1 eV, although the complex lineshapes are similar. A predicted sharp resonance near 69 eV is absent in the experimental data.

A detailed spectroscopic analysis of the resonance structure was performed in order to assign the observed features, which correspond to three Rydberg series of resonances converging to the $2s^22p^4\ ^1D_2$, $2s^22p^4\ ^1S_0$ and $2s2p^5\ ^3P$ excited states of Ne^{2+} at 44.167 eV, 47.875 eV and 66.292 eV, respectively from the ground state of Ne^+. The measurements along with their assignments are presented in Figure 2. The first two Rydberg series consist of pairs of sharp resonances separated by 97 meV that are distinguishable for autoionizing states with principal quantum numbers n as high as 25. The doubling corresponds to excitation from the ground-state and metastable-state components present in the ion beam. Resonances corresponding to the $2s2p^5(^3P)np$ series are sufficiently broad that components due to excitation from the ground and metastable states of Ne^+ are unresolved, except for the lowest 2p resonance near 42 eV.

Quantum-defect analyses were performed for each of the observed Rydberg series. The lowest members of the $2s^22p^4(^1D_2)nl$ and $2s^22p^4(^1S_0)nl$ Rydberg series were found to exhibit anomalous behavior with respect to their energy positions and relative resonance strengths, making it difficult to assign the features between 41.5 eV and 42.1 eV

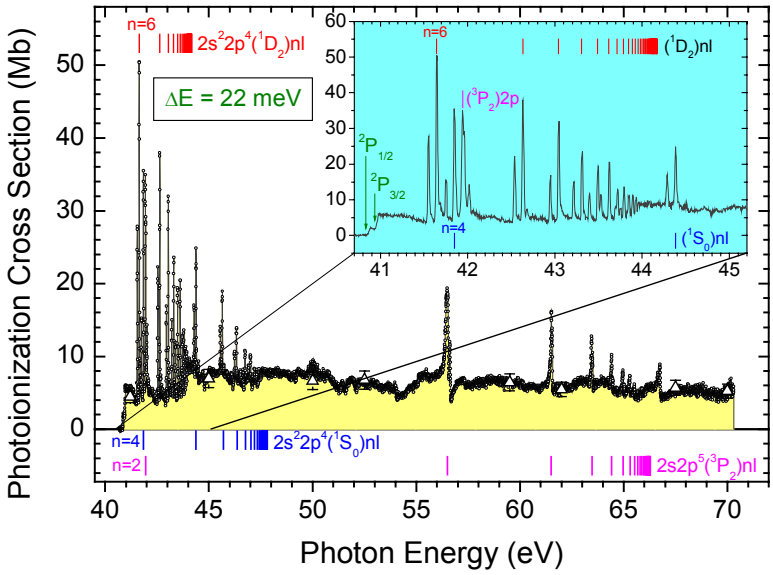

Figure 2. Absolute cross-section measurements for photoionization of Ne^{+} (triangles with error bars), to which broad photon energy scan taken at a resolution of 22 meV and a step of 4 meV was normalized. Three Rydberg series of resonances converging to excited states of Ne^{2+} are identified. The inset shows the measurements in the low-energy region on an expanded photon energy scale.

unambiguously. Each series converges to the known spectroscopic limit, independently verifying the photon energy calibration. This apparent breakdown of L-S-J coupling was not observed in photoionization of neutral fluorine [4]. It is surprising that such a dramatic change occurs suddenly along an isoelectronic sequence, motivating follow-up photoionization measurements on other members of this sequence (e.g. Na^{2+}).

REFERENCES

[1] W. Cunto, C. Mendoza, F. Ochsenbein and C. J. Zeippen, Astron. Astrophys. **275**, L5 (1993).

[2] C. A. Iglesias and F. J. Rogers, Astrophys. J. **464**, 943 (1996).

[3] A. M. Covington, A. Aguilar, I. R. Covington, M. F. Gharaibeh, C. A. Shirley, R. A. Phaneuf, I. Álvarez, C. Cisneros, G. Hinojosa, J. D. Bozek, I. Dominguez, M. M. Sant'Anna, A. S. Schlachter, N. Berrah, S. N. Nahar and B. M. McLaughlin, Phys. Rev. Lett. **87**, 243002 (2001).

[4] C. D. Caldwell and M. O. Krause, J. Phys. B Atom Molec. Phys. **27**, 4891 (1994); C. D. Caldwell, S. Benzaid, A. Menzel and M. O. Krause, Phys. Rev. A **53**, 1454 (1995).

The experimental work was supported by the Office of Basic Energy Sciences, Chemical Sciences, Geosciences and Biosciences Division, of the U. S. Department of Energy under contract DE-FG03-00ER14787 with the University of Nevada, Reno; by the Nevada DOE/EPSCoR Program in Chemical Physics and by CONACyT through the CCF-UNAM, Cuernavaca, Mexico. A.A. and M.M.SA. acknowledge support DGAPA-UNAM (Mexico) and CNPq (Brazil), respectively. The theoretical work was supported by ITAMP/Harvard-Smithsonian and by EPSRC (UK).

Principal Investigator: Ronald A. Phaneuf, Department of Physics /220, University of Nevada, Reno, NV 89557-0058. E-Mail: phaneuf@physics.unr.edu Telephone: 775-784-6818.

Transmission Functions of a Scienta SES-200 Hemispherical Analyzer.

S.E. Canton[1,2], J.D. Bozek[1], N. Berrah[2]

[1] Lawrence Berkeley National Laboratory, Advanced Light Source,
University of California, Berkeley CA 94720.
[2] Department of Physics, Western Michigan University, Kalamazoo MI 49008.

INTRODUCTION

Most of the information extracted from photoelectron spectra comes from the relative comparison of line intensities. As the range of kinetic energy in experiments carried out at synchrotron light sources is usually wide, the transmission function of the electron energy analyzer must be accounted for. The transmission functions of a Scienta SES-200 hemispherical analyzer have been determined for different pass energies (5,10,20 and 40 eV). The method is based on the measurement of the intensity ratio between photoelectron lines with dispersing kinetic energy and the corresponding Auger lines with constant kinetic energy. The standard Auger line intensities of the Xe $N_{4,5}OO$ spectrum have been obtained and used as a test of the reliability of the correction procedure.

RESULTS

The method proposed in [1] is based on the measurement of the intensity ratio between photoelectron lines and Auger lines related to the decay of the same core-hole vacancy using tunable synchrotron radiation. Because of their constant kinetic energy, the Auger lines have a constant transmission, whereas the photoline intensity reflects the relative transmission of the spectrometer.

In the present work, the transmission function F is given by the ratio of the $4d_{5/2}$ photoline in Xenon and some selected Auger lines N_5OO.

$$F_{5/2}(E_{kin}) = I_{4d_{5/2}}/(I_{51}+I_{52}+I_{53})$$

In order to include the ratio of the $4d_{3/2}$ photoline and the corresponding Auger lines N_4OO, a scaling factor R needs to be calculated using the ratio taken at high photon energy.

$$F_{3/2}(E_{kin}) = R*I_{4d_{3/2}}/(I_{41}+I_{42}+I_{43})$$

The resulting transmission curves are shown in Fig.1.

The lines were fitted with a modified Voigt profile accounting for Post Collision Interaction (PCI) distortion. All the Auger lines belonging to the same group were constrained to have equal width and asymmetry. The relative intensities once corrected agree well with the values in the literature [2].

REFERENCES

[1] J. Jauhianen J Elect Spectrosc Relat Phenom. **69** (1994) 181-187
[2] L.O. Werme et al, Phys. Scr. **6** (1972) 141

This work was funded by the Department of Energy, Office of Science, Basic Energy Sciences, Chemical and Material Science Division, under the contract No. DE-AC03-76SF00098.

Principal investigator: Nora Berrah, Physics Dept., Western Michigan University, 616-387-4955, berrah@wmich.edu.

Fig.1 Transmission functions for 5, 10, 20 and 40 eV pass energy.

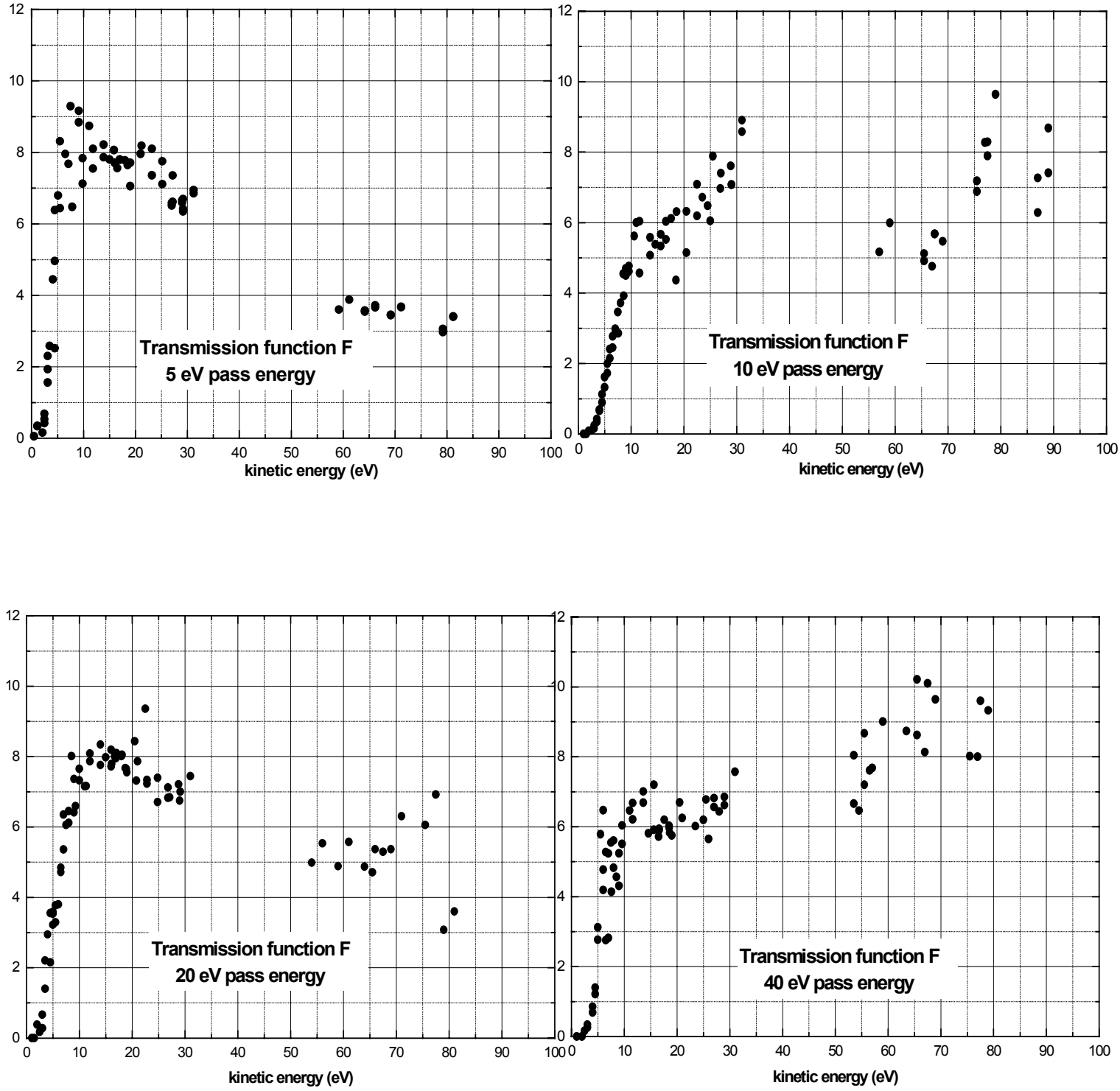

Vibrationally resolved resonant Auger spectroscopy of formaldehyde at the C$1s^{-1}\pi^*$ resonance.

J.D. Bozek[1], S.E. Canton[1,2], E. Kukk[3] and N. Berrah[2]
[1] Lawrence Berkeley National Laboratory, Advanced Light Source, University of California, Berkeley CA 94720.
[2] Department of Physics, Western Michigan University, Kalamazoo MI 49008.
[3] Department of Physical Sciences, Oulu University, Linnanmaa, Oulu FIN-90570, Finland.

INTRODUCTION

Resonant Auger (RA) spectroscopy has benefited greatly from advances in both light sources and electron spectrometer techniques in the past decade. Transitions to molecular orbitals are particularly interesting to study using RA spectroscopy due to the dynamics induced in the excited state. When it is not dissociative, changes in the molecular geometry induced by the excitation allow the RA decay process to sample different parts of the potential energy surface of the molecule that can not be accessed directly by single photon absorption and extensive vibrational structure is often observed in the participator decay. Such studies have been performed with vibrational resolution for a number of simple diatomic or triatomic [1,2] molecules and start being explored for larger molecules. In this work, vibrationally resolved RA spectra of gaseous formaldehyde have been measured under resonant Raman conditions at several photon energies on the C$1s^{-1}\pi$ resonance. Utilizing high-resolution photoexcitation, specific vibrational states of the C$1s^{-1}\pi^*$ resonance were selectively populated. Participator Auger decay of the excited state populates mainly the A-D ionic states, without any discernable increase in the intensity of the X state. The vibrational manifold of the A state band was examined in details for resonant and non-resonant photoionization. The observations are attributed to changes in the potential energy surfaces.

EXPERIMENT

The experiments were carried out on beamline 10.0.1, which delivers more than 10^{12}photons/sec in 0.1% bandwidth. The photoelectron spectra were measured with a GammaData Scienta SES-200 hemispherical analyzer in a spectrometer system developed exclusively for gas phase experiments. Monomeric formaldehyde in the gas phase was obtained by heating to 70^0C the sample cell containing the dimerized form paraformaldehyde (Aldrich, 96% purity). The presence of monomeric formaldehyde and its purity were verified by measuring the outer valence photoelectron spectrum.

RESULTS

A low-energy electron yield spectrum of the C$1s^{-1}\pi^*$ resonance shown in Fig.1 was first measured with the present apparatus to provide good calibration of the energy scale for the subsequent RA measurements. This spectra gives also an idea of the extent of excitation for each normal mode ν_1 mostly C-H stretching, ν_2 C=O mostly stretching, ν_3 mostly HCH bending (Table 1). Vibrationally resolved RA spectra were recorded at the energies corresponding to the positions indicated on Fig.1.and are shown of Fig.2. RA spectra a-c were measured at photon energies corresponding to the excitation of primarily ν_2 quanta in the excited state. The position of the peak intensity steadily increases through higher vibrational levels in the ionic state as higher ν_2 vibrational levels are accessed in the core excited state. The trend continues for spectra d-f although the vibrational levels populated in the excited state become less clear due to the probability of exciting mixtures of quanta ν_1 and ν_3. This behavior can be qualitatively explained: the change from spectrum a to c is mainly due to the excitation of the higher levels of the ν_2 manifold of the A state, as the vibrational transitions originate from the ν_2=0,1,2 levels of the core excited state respectively. Consequently, the maximum intensity shifts from the ν_2=0 (spectrum a) to the ν_2=2 level (spectrum c) of the final ionic state A. The spectrum has quite different appearance, as now the vibrational transitions originate from the ν_1=1 level, but the ν_2=2 manifold again comes from the ground level of the core excited state (as for spectrum a). Thus the ν_2=0 final state is again populated strongly, but the intensity is shifted to the higher levels in the ν_1 final state manifold. The next spectra e and f again display changes due to the intensity moving to the higher levels of the manifold. The vibrational states populated in the B state band are less obvious owing to the band's lower intensity, but similar trends are discernable. The dispersion of the vibrational intensity A and B state can be attributed to geometric changes in the potential energy surfaces (PES). Geometric changes in the H_2CO molecule upon excitation were reported by analysis of photoabsorption spectrum [3]. The C=O bond increases, while the

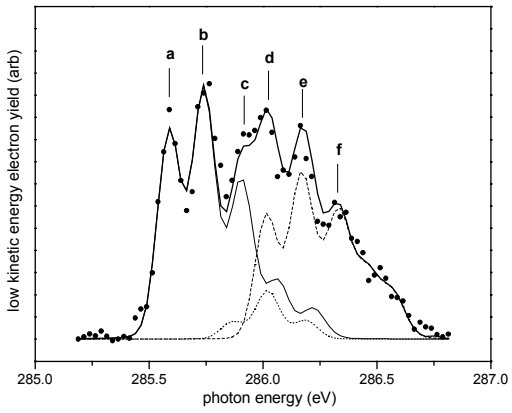

FIG.1 : Low energy electron yield of the $C1s^{-1}\pi^*$ resonance in formaldehyde measured with 75 meV photon resolution. The experimental data has been deconvoluted into contributions from different vibrational states using parameters from [3]. The positions where resonant Auger spectra were measured are indicated by the letters a-f.

C-H bond contracts. The A RA final state, results from the removal of a C=O bond in the ionic state and as such, the resonant decay occurs between two states with similarly displaced PES. Hence the ν_2 vibrational quantum number of the excited state is preserved in the ionic state and reflected in the vibrational populations in the participator Auger decay lines. The ν_1 progression is very strong, however, indicating that there is a large change in the C-H bond distance between the core excited and A ionic state

TABLE 1: Photon energies of the positions indicated of Fig. 1,where resonant Auger spectra were measured, and relative contributions of different vibrational levels to the $C1s^{-1}\pi^*$ band at those energies.

Label	Photon Energy	Vibrational State Contribution (total = 100)
a	285.59	(0,0,0) – 100
b	285.74	(0,1,0) – 100
c	285.89	(0,2,0) – 82 (0,0,1) – 10 (1,0,0) – 8
d	286.02	(1,0,0) – 52 (0,1,1) – 20 (0,3,0) – 14 (0,4,0) - 14
e	286.17	(1,1,0) – 76 (0,4,0) – 8 (0,5,0) – 8 (0,2,1) – 8
f	286.32	(1,2,0) – 78 (1,0,1) – 14 (1,1,1) – 8

REFERENCES

[1] Kukk et al, Phys. Rev. A **62** (2000) 032708/1-9
[2] Miron et al J. Electron Spectrosc. Relat. Phenom. **93**, 95 (1998)
[3] Remmers et al, Phys. Rev. A **46**, 3945 (1996)

This work was funded by the Department of Energy, Office of Science, Basic Energy Sciences, Chemical and Material Science Division, under the contract No. DE-AC03-76SF00098.

Principal investigator: Nora Berrah, Physics Dept., Western Michigan University, 616-387-4955, berrah@wmich.edu.

ACKNOWLEDGEMENTS

We are indebted to Bruce Rude for his outstanding technical assistance and the staff of the ALS for their excellent operation of the facility.

FIG. 2 : Vibrationally resolved resonant Auger spectra of the participator decay states of formaldehyde measured at the positions indicated on Fig.1 and in Table1.